2021

Retinal cytoarchitectural changes in schizophrenia and bipolar disorder: a meta-analysis and exploratory study

BOSTON UNIVERSITY

SCHOOL OF MEDICINE

Thesis

RETINAL CYTOARCHITECTURAL CHANGES IN SCHIZOPHRENIA AND BIPOLAR DISORDER: A META-ANALYSIS AND EXPLORATORY STUDY

by

DEEPTHI BANNAI

B.S., The University of Texas at Austin, 2017
B.S.A., The University of Texas at Austin, 2017

Submitted in partial fulfillment of the

requirements for the degree of

Master of Science

2021

Approved by

First Reader

Manju L Subramanian, M.D.
Associate Professor of Ophthalmology

Second Reader

Paulo Lizano, M.D., Ph.D.
Instructor of Psychiatry
Beth Israel Deaconess Medical Center, Harvard Medical School

ACKNOWLEDGMENTS

I would like to sincerely thank my readers, Dr. Manju Subramanian and Dr. Paulo Lizano, for their invaluable guidance and feedback for my thesis work. Furthermore, I am extremely grateful to Dr. Lizano for his mentorship and encouragement, without which I would not have been able to navigate this project or cultivate meaningful research skills. In addition, I would like to thank Dr. John B. Miller and Megan Kasetty for their assistance and guidance for the retinal scans as well as Olivia Lutz and Rachal Hegde for their never-ending advice and friendship. I would like to thank Dr. Matcheri Keshavan for the opportunity of working in his lab and for the generous use of his BSNIP-2 dataset and neuroimaging resources. Finally, I would like to thank my family and their continuous support in my academic endeavors.

RETINAL CYTOARCHITECTURAL CHANGES IN SCHIZOPHRENIA AND BIPOLAR DISORDER: A META-ANALYSIS AND EXPLORATORY STUDY

DEEPTHI BANNAI

ABSTRACT

Introduction: Schizophrenia (SZ) and bipolar disorder (BD) are neurodegenerative psychotic disorders hallmarked by reductions in gray and white matter volume. Limitations in neuroimaging have led to the use of OCT to study retinal layer biomarkers and their relation to brain pathology. This thesis includes a meta-analysis of current literature and an exploratory analysis of retinal layer thickness in relation to SZ and BD.

Methods: For the meta-analysis, twelve articles were identified using PubMed, Web of Science, and Cochrane database. Diagnostic groups were proband (SZ and BD combined), SZ only, BD only, and healthy control (HC) eyes. Analyses utilized fixed and random effects models, in addition to assuring that bias was adjusted for and that results were cross-validated. Statistical analyses were performed using the "meta" package in R, with results reported as standard mean differences (SMD). The exploratory analysis included a total of 38 subjects (24 probands and 14 HC). Retinal measures were co-varied for age, sex, race, body mass index (BMI), and best-corrected visual acuity (BCVA). Correlations between retinal and clinical and cortical measures were also performed. Clinical data included illness duration, symptom severity, antipsychotic dosage, and smoking status. Neuroimaging data included gray matter (GM) thickness, gray matter volume, and intracranial volume (ICV). Linear

effects and mixed effects models were used to study mean eye and right/left eye measures, respectively. Statistical analysis was done in R.

Results: A total of 820 patient eyes (541 SZ and 279 BD) and 904 HC eyes were used for the meta-analysis. Compared to HC eyes, probands, SZ, and BD eyes showed significant thinning the peripapillary retinal nerve fiber layer (RNFL), with atrophy greatest in the nasal, temporal, and superior regions. In addition, all diagnostic groups demonstrated significant reductions in the combined ganglion cell layer and inner plexiform layer (GCL-IPL) compared to HC. No significant differences were found for choroidal and macular measures. No significant relationships were seen from meta-regression analysis for clinical measures. For the exploratory analysis, retinal measures from a total of 24 probands (18 SZ and 6 BD) and 14 HC was studied. Compared to HC, probands showed reductions in overall RNFL in mean eye measures, while increases in the inner and outer RNFL were seen in left eye measures. No significant group differences were seen in the GCL, IPL, and inner nuclear layer (INL). The outer plexiform layer (OPL) showed significant thickening in probands and SZ compared to HC for all eye measures. Probands showed trending reductions in the outer nuclear layer (ONL) in the left eye compared to HC. No significant correlations were found between retinal layers and illness duration, overall PANSS (Positive and Negative Syndrome Scale) score, PANSS negative symptom subscore, and smoking status. PANSS positive symptom subscore showed significant and trending negative correlations to the RNFL and GCL, respectively. Antipsychotic medication dosage displayed a trending negative relationship with the IPL. GM thickness showed a significant and trending negative correlation to the RNFL and ONL, respectively. Furthermore, a trending inverse

relationship was observed between GM volume and the OPL. Finally, ICV demonstrated a trending and significant negative relationship with GCL and OPL thickness, respectively. **Conclusion:** The meta-analysis showed that atrophy in RNFL and GCL-IPL measures are widely associated with psychosis. Furthermore, it supports previous findings of gray and white matter reductions in SZ and BD. The exploratory analysis showed psychosis-associated reductions in the RNFL and ONL layers, consistent with previous literature. Contradictory findings, the thickening of the ONL, can be attributed to the conflicting findings, but might also be explained by neuro-inflammatory pathways related to psychotic disorders.

TABLE OF CONTENTS

LIST OF TABLES

LIST OF FIGURES

LIST OF ABBREVIATIONS

AA ..... African American

AMD ..... Age-related Macular Degeneration

BCVA ..... Best-Corrected Visual Acuity

BBB ..... Blood Brain Barrier

BMI ..... Body Mass Index

BD ..... Bipolar Disorder

CA ..... Caucasian

CGI ..... Clinical Global Impression

CI ..... Confidence Interval

CT ..... Choroidal Thickness

DR ..... Diabetic Retinopathy

ELM ..... External Limiting Membrane

FDR ..... False Discovery Rate

GCC ..... Ganglion Cell Complex

GCL ..... Ganglion Cell Layer

GM ..... Gray Matter

HC ..... Healthy Controls

ICV ..... Intracranial Volume

ILM ..... Inner Limiting Membrane

INL ..... Inner Nuclear Layer

IPL ..... Inner Plexiform Layer

LGN ..... Lateral Geniculate Nucleus

MS ..... Multiple Sclerosis

MT ..... Macular Thickness

MV ..... Macular Volume

ONL ..... Outer Nuclear Layer

OPL ..... Outer Plexiform Layer

OT ..... Other

PANSS ..... Positive and Negative Syndrome Scale

PRISMA ..... Preferred Report Items for Systematic Reviews and Meta-Analyses

RPE ..... Retinal Pigmented Epithelium

RNFL ..... Retinal Nerve Fiber Layer

SAD ..... Schizoaffective Disorder

SD-OCT ..... Spectral Domain Optical Coherence Tomography

SMD ..... Standardized Mean Difference

SS-OCT ..... Swept Source Optical Coherence Tomography

SZ ..... Schizophrenia

TD-OCT ..... Time Domain Optical Coherence Tomography

VA ..... Visual Acuity

Young Mania Rating Scale ..... YMRS

INTRODUCTION

Schizophrenia and Bipolar Disorder

Schizophrenia (SZ) and bipolar disorder (BD) are serious and progressive mental illnesses characterized by cognitive, functional, and social deficits. Both present in late-adolescence or early adulthood and demonstrate psychotic or manic symptoms (American Psychiatric Association, 2013; Merikangas et al., 2007). Symptoms of schizophrenia are categorized as either positive or negative. Positive symptoms include delusions, hallucinations, and disorganized thoughts and behavior, while negative symptoms comprise of flat affect, alogia (difficulty with speaking), and avolition (inability to initiate or perform goal-directed behavior). In bipolar disorder, there is an alternation between episodes of mania and episodes of depression (American Psychiatric Association, 2013). The pathophysiology of either disorder is not entirely known, but recent studies have shown that they share a similar pathophysiology. These similarities include gray and white matter atrophy, glial cell dysfunction, and increased inflammatory markers (DeLisi et al., 2006; Kempton et al., 2008; Moorhead et al., 2007; Najjar et al., 2013). Therefore, imaging techniques studying the brain, structural magnetic resonance imaging (MRI), and the eye, retinal optical coherence tomographic (OCT), can help to illuminate the general underlying neurobiology and pathological mechanisms of psychosis.

While advancements have been made to understand SZ and BD with neuroimaging techniques, there are limitations. Image resolution, cost, and accessibility to certain brain regions limit what information researchers can collect and analyze. Because of this, OCT

analysis of retinal cell layers has been gaining traction as a non-invasive and high-resolution tool to study new biomarkers in neurological disorders (London et al., 2013).

Optical Coherence Tomography

OCT was first developed in the 1990s as an *in-vivo* imaging technique. It works similarly to ultrasound, utilizing backscattered light to form a 2D, real-time image of tissue (Huang et al., 1991). Over time, OCT has become the standard of care for imaging of the optic nerve and macular region of the retina, and it is used for the diagnosis of various ophthalmic diseases, most commonly age-related macular degeneration (AMD) and diabetic retinopathy (DR) (Das, 2016; de Barros Garcia et al., 2017). Retinal OCT imaging has also been utilized in the study of neurological disorders that have associated vision loss, such as Alzheimer's Disease, Parkinson's Disease, and Multiple Sclerosis (MS) (Almarcegui et al., 2010; Lu et al., 2010; Yu et al., 2014). These studies have shown the efficacy of OCT imaging in understanding both underlying neurodegenerative pathways as well as providing potential early diagnoses. Finally, investigations into stroke and cardiovascular disease (such as myocardial infarction) have demonstrated links with impaired retinal architecture (Kromer et al., 2018; Osiac et al., 2014).

Some studies have analyzed alterations in retinal thickness and volume in SZ and BD, with particular interest in the retinal nerve fiber and ganglion cell layers (Mehraban et al., 2016; Steven M. Silverstein et al., 2017). Advances in OCT technology from the first-generation time domain (TD) OCT to spectral domain (SD) and swept source (SS) OCT have greatly improved spatial resolution of the images and have allowed for examination into deeper retinal layers which had not been widely analyzed due to poor segmentation.

The Visual Pathway

Because the retina shares embryological origins with the brain, it has been increasingly studied as a "window" into the underlying pathophysiology of neurologic disorders (Chu et al., 2012; Mancall & Gray, 2011).

The retina is the sensory neural layer of the eye and functions to detect and provide initial analysis of visual information. It contains 6 cell types and 10 layers (Figure 2). From the vitreous body, the layers are as follows: internal limiting membrane (ILM), retinal nerve fiber layer (RNFL), ganglion cell layer (GCL), inner plexiform layer (IPL), inner nuclear layer (INL), outer plexiform layer (OPL), outer nuclear layer (ONL), external limiting membrane (ELM), photoreceptor layer, and retinal pigmented epithelium (RPE). The ILM acts as the the glial boundary between the retina and vitreous body, while the ELM is a junction between the processes of glial cells and photoreceptor cell processes. The RPE forms a tight boundary against the choroid, preventing any fluid from the capillary beds from leaking into the retina.

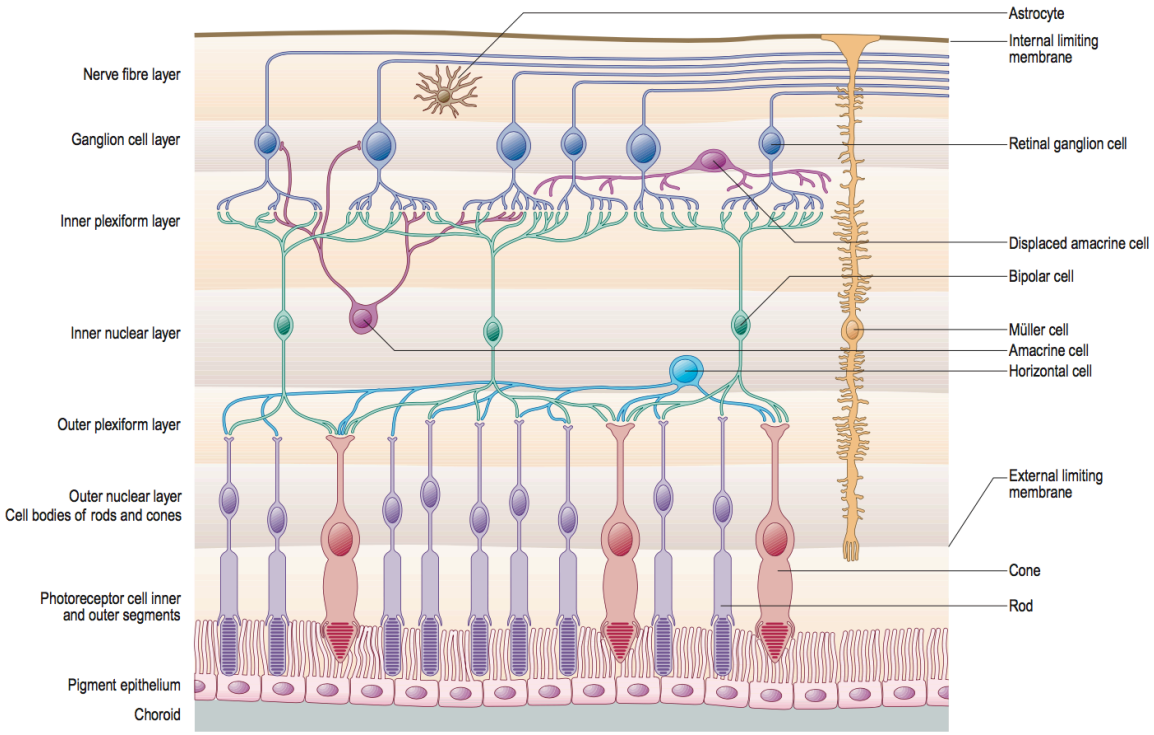

Figure 1: Retinal layer diagram. Illustration of the retinal layers and cell types. From *Gray's Clinical Neuroanatomy: The Anatomic Basis for Clinical Neuroscience*.

As light enters the eye, it travels through all the layers of the transparent retina to the photoreceptors, whose cell bodies are contained within the ONL. There are two types of photoreceptors: rods and cones. Rods are responsible for low-light (scoptic) vision, but have low spatial acuity and do not facilitate color vision. Cones come in three types, red, blue, and green, and allow for photopic vision: high spatial resolution and color vision in well-lit conditions. From there, the visual signal is transmitted to the synaptic arrangements between photoreceptor, bipolar, and horizontal cells of the OPL. Bipolar and horizontal cells are interneurons, and respectively, they function to help transmit signals from the photoreceptor cells to the ganglion cells and to facilitate connections between rod and cone photoreceptor cells. After the OPL are the cell bodies of the amacrine, bipolar, and horizontal cells in the

INL. These cells forward the visual signal to the IPL and across synapses between the axons of bipolar cells and dendrites of ganglion cells.

The GCL comprises of the cell bodies of ganglion cells and nuclei of amacrine cells. The unmyelinated axons of the ganglion cells make up the RNFL, and these fibers coalesce at the optic nerve and primarily to the lateral geniculate nucleus (LGN) of the thalamus.

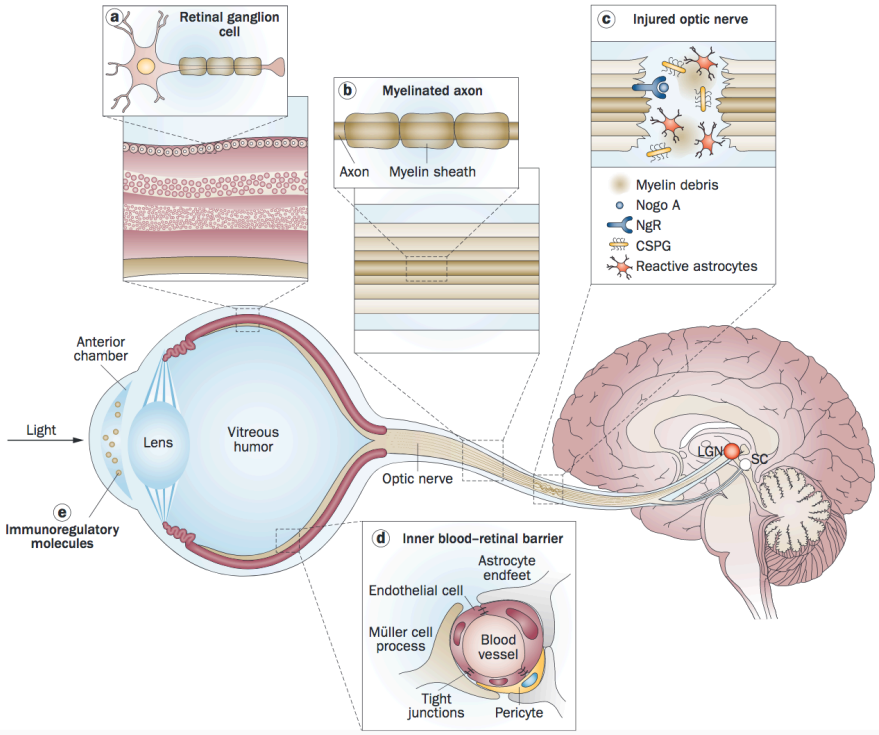

Figure 2: Connections between the eye and the brain. From *The retina as a window to the brain – from eye research to CNS disorders.*

Visual Deficits in Psychosis

SZ and BD are associated with vision deficits and aberrations in the visual pathway. Perceptual organization, the ability to group data into patterns, has been shown to be impaired in SZ, manifesting as difficulty in processing facial cues, social cognition, working memory, and selective attention (Silverstein & Keane, 2011). In a review by Chen et al. (2011), poor spatial and temporal eye-tracking (motion processing) has been associated with

SZ. Furthermore, SZ and BD have been linked with deficits in emotional facial feature recognition (Schaefer et al., 2010; Turetsky et al., 2007). Abnormal visual motion perception has also associated with BD, along with visual masking impairments (Chkonia et al., 2012; O'Bryan et al., 2014). Literature analyzing the cognitive aspects of visual deficits in SZ and BD are extensive, but

further research is warranted into related neurobiological mechanisms.

The aim of this thesis is two-fold: to conduct a meta-analysis of current literature on retinal imaging biomarkers in SZ and BD and to undergo an exploratory analysis on a sample of participants with SZ and VD. The meta-analysis incorporates materials from a published co-first author paper (Lizano et al., 2020), where the thesis author made significant research and writing contributions. This meta-analysis will summarize current literature in the field, describe gaps in understanding, and uncover areas of analysis for use in the exploratory study. The aim of the exploratory analysis is to illuminate aberrant retinal cytoarchitecture and associations to cortical and clinical measures in SZ and BD. Because the RNFL contains fibers that form the optic nerve and the GCL contains the ganglion cell bodies, we hypothesize that thinning would be seen in these layers leading to overall retinal thickness reductions. Furthermore, we hypothesize that positive correlations would be seen between cortical measures and retinal layer thicknesses, as gray and white matter integrity would correlate with that of the retinal layers.

METHODS

Meta-Analysis

This section has been adapted from the author's co-first author publication: Lizano, P., Bannai, D., Lutz, O., Kim, L. A., Miller, J., & Keshavan, M. (2020). A Meta-analysis of Retinal Cytoarchitectural Abnormalities in Schizophrenia and Bipolar Disorder. *Schizophrenia Bulletin*, *46*(1), 43–53. https://doi.org/10.1093/schbul/sbz029.

Study Selection

Two investigators (PL and DB) comprehensively searched and identified retinal OCT SZ and BD studies through PubMed, Web of Science, and the Cochrane Collaboration's Database of Systematic Review in July 2018 and again in December 2018. The Preferred Report Items for Systematic Reviews and Meta-Analyses (PRISMA) guidelines were followed (Appendix Table 1; Moher, Liberati, Tetzlaff, & Altman, 2009). Search strategies used were "schizophrenia OR psychosis OR bipolar disorder" AND "optical coherence tomography OR retinal nerve fiber layer thickness OR macula volume OR ganglion cell layer OR choroidal layer". Manual evaluation of citations from selected papers added more relevant studies. Articles were screened for eligibility via inclusion and exclusion criteria. Inclusion criteria for studies were:

1. OCT assessment in patients with a diagnosis of SZ or BD defined by the DSM-4, Diagnostic Interview for Psychosis (DIP), or a psychiatrist (American Psychiatric Association, 2013)
2. Cross-sectional or prospective studies
3. Pertinent data within article or available upon request

4. English language

Articles were excluded if they fit one or more of the exclusion criteria:

1. No control group
2. No peripapillary RNFL thickness measurements
3. Significant overlap in study population
4. Data measurements were in a different format than mean and standard deviation values

Assessment of Quality

The Newcastle-Ottawa Scale (NOS) provided a structured format in order to evaluate the strength of articles included in meta-analysis based on selection of the study groups, comparability of groups, and data measure parameters. An overall quality score was defined as the number of criteria met by each study and was done by the two raters, PL and DB (Wells et al., 2012).

Pilot Study

Subjects

A total of 38 participants with SZ (n =11), schizoaffective disorder (SAD, n = 7), BD (n = 6), and healthy controls (HC, n = 14) were included for a preliminary analysis of retinal segmentation in psychosis. The diagnostic groups were well matched for age, race, best-corrected visual acuity (BCVA), right visual acuity (VA), and left VA. BCVA is the visual acuity measured when participants wore their normal corrective glasses or lenses. Smoking

status was measured using the Fagerstrom Test for Nicotine Dependence (FTND), where answers to six yes or no questions are rated (Fagerström, 1978). The sum of the scores from this test was used as the smoking status clinical measure. Scores for the Positive and Negative Syndrome Scale (PANSS), a medical scale used to measure symptom severity in patients with schizophrenia, were available for 16 of the 24 probands (Kay et al., 1987).

OCT Data

Retinal OCT scans were acquired at Massachusetts Eye and Ear Institute using a Heidelberg Spectralis SD-OCT scanner. In addition, OCT angiography (OCT-A) images were collected with a Triton DRI-OCT swept source scanner with a 6x6mm grid centered on the fovea. An Early Treatment Diabetic Retinopathy Study (ETDRS) grid, shown in Figure 3, was centered around the fovea and used to collect information in a central region and inner and outer rings.

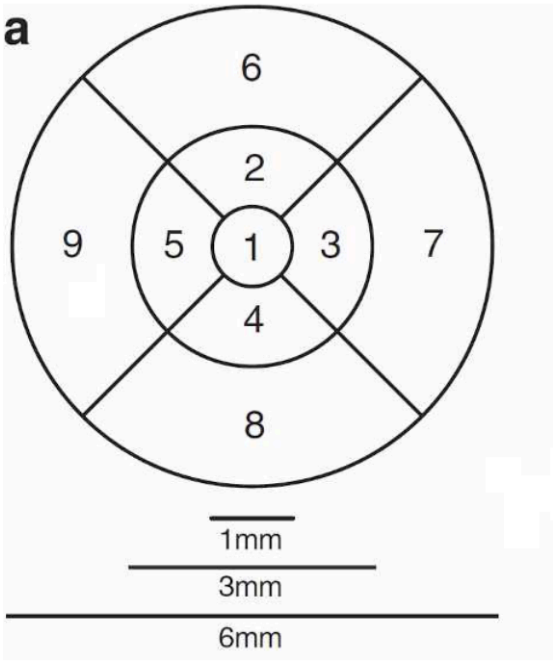

Figure 3: Illustration of the ETDRS grid. Regions marked (1) comprise the central region. Regions marked (2)-(5) comprise the inner ring, and regions (6)-(9) make up the outer ring. Figure taken from (Demirkaya et al., 2013).

MRI

Structural T1-weighted magnetization prepared rapid gradient echo (MPRAGE) images were gathered using a General Electric 3 Tesla scanner. Freesurfer 6.0 was used to pre-process the structural images and to parcel out various cortical structures and their measures. The three cortical markers utilized in the pilot study were gray matter (GM) thickness, GM volume, and total intra-cranial volume (ICV).

Statistical Analysis

The meta-analysis was conducted using RStudio software and the 'metafor' package. Meta-regression analysis utilized the 'metareg' package. For the pilot study, independent sample t-tests were used to compare demographics. Eye data was collected from each eye, right (OD)

and left (OS), and mean values for each region were calculated by combining OD and OS measures. Analysis using the mean eye segmentation values were run with linear model to assess differences in retinal layer thicknesses. A linear mixed effects model was utilized for individual eye data, with fixed effects being age, sex, race, BMI, and BCVA. Because segmentation data within each patient varied between each eye, the segmentation data for the other eye was used as the random effect. Statistical analyses were done using RStudio software.

RESULTS

Meta-Analysis

This section, including Figures 4-10 and Table 1, has been adapted from the author's co-first author publication: Lizano, P., Bannai, D., Lutz, O., Kim, L. A., Miller, J., & Keshavan, M. (2020). A Meta-analysis of Retinal Cytoarchitectural Abnormalities in Schizophrenia and Bipolar Disorder. *Schizophrenia Bulletin*, *46*(1), 43–53. https://doi.org/10.1093/schbul/sbz029.

Selected Studies

Figure 4 summarizes the selection of studies for this meta-analysis. One hundred and eighty-two papers were identified from searching through online databases, and one paper was found from an outside source. Seventy-four articles remained after removal of duplications, and twenty-two of those were full-text papers. From there, 10 were excluded: two papers were commentary, five overlapped with other papers, one had a sample size (SZ or BD) less than 10 subjects, one was a retinal vascular study, and one did not contain necessary data for analysis. Twelve studies were eligible for qualitative and quantitative meta-analysis, containing a pooled sample of 521 probands (315 SZ and 206 BD) and 496 healthy controls. After selection, two independent raters, DB and PL, utilized the Newcastle Ottawa Scale to assess the quality of each study, shown in Table 1. Table 1 also includes other data parameters such as diagnostic criteria, number of eye hemispheres with data published, and demographics data for patient and control groups. An intra-class correlation (ICC) analysis was performed to test the rater reliability. NOS scores were above 6 for all studies, with a

mean score of 6.63. Finally, the ICC value was 0.835, with a confidence interval from 0.53 to 0.96 and $p<0.001$.

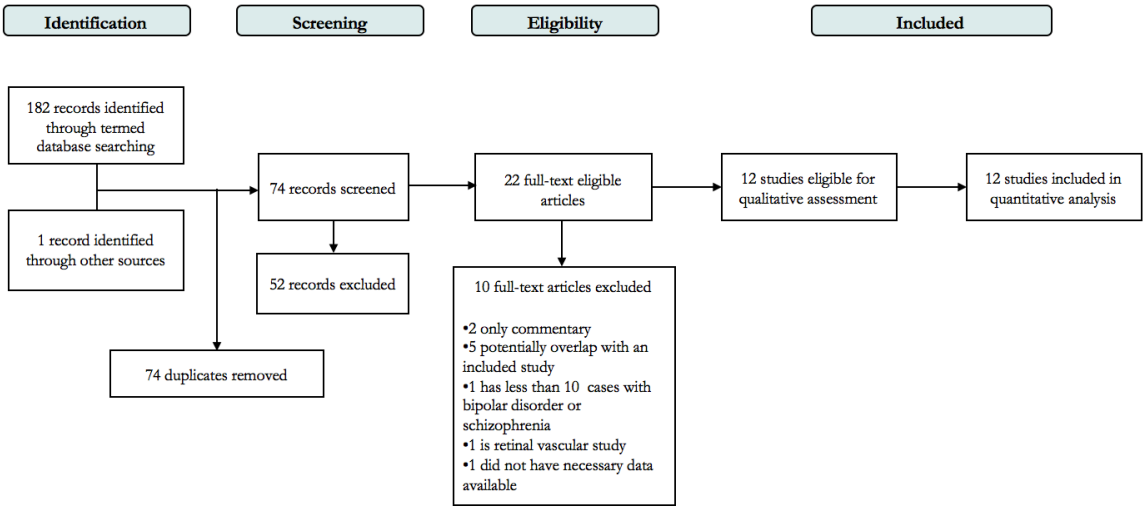

Figure 4: Meta-analysis study selection.

Table 1: Meta-analysis study characteristics.

			Patients			Controls											
Study	Diagnosis	Eyes	n	Women (%)	Age (years)	n	Women (%)	Age (years)	Diagnostic Criteria	Level of Care	Illness Stage	Disease Duration (years)	Symptom Severity Score	Medication Status	OCT device	Technique	NOS PL/DB
Ascaso et al (2015)	SZ	2	30	23.0%	45.1 (10.4)	30	27.0%	44.5 (10.9)	DSM-IV	IP	Chronic	16.3 (11.2)	PANSS 101.4 (27.7)	Medicated	Stratus (Carl Zeiss)	TD-OCT	7/7
Celik et al (2016)	SZ	1	81	20.0%	35.6 (10.1)	41	31.7%	35.5 (15.9)	DSM-IV	OP	Chronic	13.3 (9.2)	PANSS 73.6 (19.8)	Medicated	Spectralis OCT (Heidelberg)	SD-OCT	6/6
Chu et al (2012)	SZ	2	49	26.5%	29.9 (8.7)	40	37.5%	29.5 (6.1)	DIP	OP	FEP	4.4 (3.6)	SANS 3.7 (0-16) SAPS 2 (0-10)	Medicated	Stratus OCT3 (Carl Zeiss)	TD-OCT	7/7
Lee et al (2013)	SZ	1	30	40.0%	37.2 (10.7)	30	53.3%	35.9 (9.1)	DSM-IV	IP, OP	Acute, Chronic	0-10	NA	Medicated	Cirrus OCT 4000 (Carl Zeiss)	SD-OCT	7/7
Silverstein et al (2017)	SZ	2	32	41.0%	40.5 (12.1)	32	44.0%	39.2 (11.0)	DSM-IV	OP	Chronic	NA	NA	Medicated	Cirrus OCT 4000 (Carl Zeiss)	SD-OCT	6/7
Yilmaz et al (2016)	SZ	2	34	26.5%	39.9 (10.3)	30	33.3%	38.6 (9.6)	NA	OP	Chronic	NA	NA	NA	Cirrus OCT 4000 (Carl Zeiss)	SD-OCT	6/6
Topcu-Yilmaz et al (2018)	SZ	1	59	45.8%	36.6 (9.5)	37	59.5%	32.1 (12.3)	DSM-IV	IP	Acute, Chronic	10.3	PANSS 75.2 (20.1)	Medicated	Spectralis OCT (Heidelberg)	SD-OCT	6/6
Garcia-Martin et al (2018)	BD euthymic	1	30	40.0%	49.7 (11.2)	80	46.3%	49.9 (8.8)	DSM-IV	OP	Chronic	16.5 (6.3)	NA	Medicated	Spectralis OCT (Heidelberg)	SD-OCT	6/6
Kalenderoglu et al (2016)	BD euthymic	2	43	46.5%	35.6 (10.5)	43	44.2%	40.5 (15.5)	DSM-IV	OP	Chronic	6.8 (10.6)	NA	Medicated	Spectralis OCT (Heidelberg)	SD-OCT	7/7
Khalil et al (2017)	BD non-euthymic	1	80	47.5%	30.9 (9.3)	80	42.5%	32.9 (8.7)	DSM-IV	IP	Acute	NA	NA	Medicated	SITA (Carl Zeiss)	SD-OCT	7/7
Mehraban et al (2016)	BD non-euthymic	2	30	20.0%	33.8 (9.2)	30	20.0%	31.2 (9.5)	DSM-IV	IP, OP	Acute, Chronic	10.6 (8.6)	NA	NA	3D OCT-1000 (Topcon)	SD-OCT	7/7
Polo et al (2018)	BD euthymic	1	23	65.2%	49.7 (8.8)	23	65.2%	49.0 (9.4)	DSM-IV	OP	Chronic	16.1 (6.7)	NA	Medicated	DRI Triton OCT (Topcon)	SS-OCT	7/7

Note: Data are presented as mean (standard deviation). SZ, schizophrenia; BD, bipolar disorder; DSM, Diagnostic and Statistical Manual; DIP, Diagnostic Interview for Psychosis; PANSS, Positive and Negative Symptom Scale; SAPS, Scale for the Assessment of Positive Symptoms; SANS, Scale for the Assessment of Negative Symptoms; IP, inpatient; OP, outpatient; OCT, Optical Coherence Tomography; TD, Time Domain; SD, Spectral Domain; SS, Swept Source; NOS, Newcastle-Ottawa Scale; PL/DB, study authors.

Differences in Peripapillary RNFL

The peripapillary RNFL was studied in overall and subfield regions. For overall peripapillary RNFL, there were twelves studies analyzed with a total of 820 eyes from probands (541 SZ and 279 BD) and 904 eyes from healthy controls (HC, 575 from SZ and 329 from BD studies). A significant reduction of thickness in the overall peripapillary RNFL was seen in probands (SMD = -0.74, CI = -1.15 to -0.33, p = 0.002), SZ (SMD = -0.51, CI = -0.85 to -0.17), and BD (SMD = -1.06, CI = -2.11 to 0) eyes compared to controls (Figure 5). The funnel plot, indicating whether or not publication bias is present in the sample, did not indicate any bias upon qualitative assessment (Appendix Figure 1A). Meta-regression analysis of age, sex, disease duration, OCT device, and NOS score did not show confounding effects with layer thickness (Appendix Table 1). Covariates such as severity of psychosis, smoking status, and antipsychotic dosage did not have meta-regressions performed as the sample sizes were not large enough.

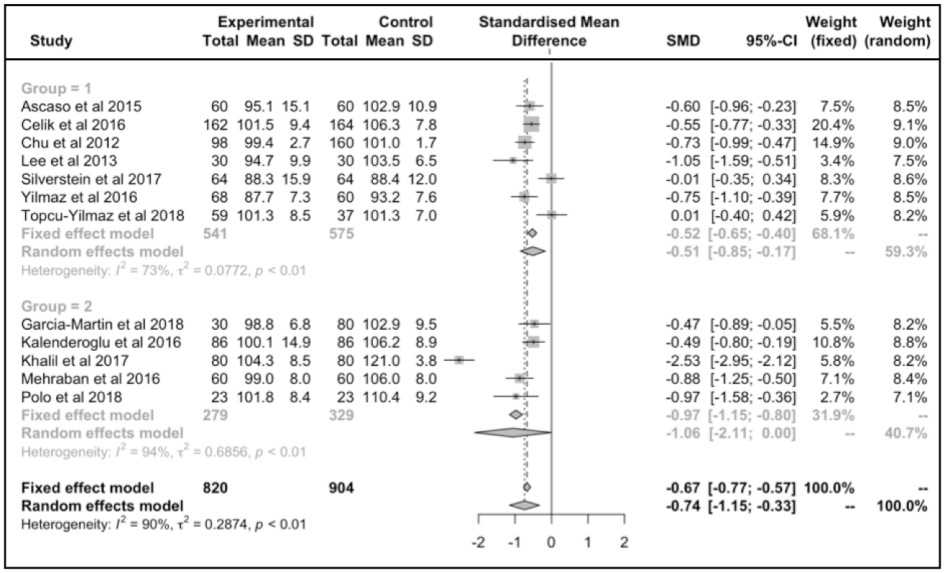

Figure 5: Meta-analysis data for overall peripapillary RNFL. Forest plots with fixed and random effects as well as standardized mean difference (SMD) are given for RNFL data in probands, SZ (group 1) and BD (group 2). "Total" indicates the number of eyes whose measures are used to calculate mean

difference. Horizontal bars in the forest plot indicate the 95% confidence intervals (CI). Size of the square indicates the weight for each study.

The same twelve studies included measurements for nasal and temporal peripapillary RNFL thickness. Compared to HC, there was significant thinning in the nasal RNFL in probands (SMD = -0.26, CI = -0.36 to -0.17, $p < 0.001$), SZ (SMD = -0.28, CI = -0.52 to -0.04), and BD (SMD = -0.25, CI = -0.41 to -0.09) eyes (Figure 6A). The funnel plot indicated no publication bias (Appendix Figure 1B). For the temporal RNFL, significant thinning was seen in proband (SMD = -0.23, CI = -0.40 to -0.06, $p < 0.001$) and SZ (SMD = -0.19, CI = -0.31 to -0.07) eyes, but not for BD eyes (SMD = -0.28, CI = -0.67 to 0.10, Figure 6B). Trim and fill method analysis was utilized to correct for publication bias observed in the funnel plot. Only the effect for probands remained significant after this correction (SMD = -0.20, CI = -0.37 to -0.034, $p = 0.023$, Appendix Figure 1C).

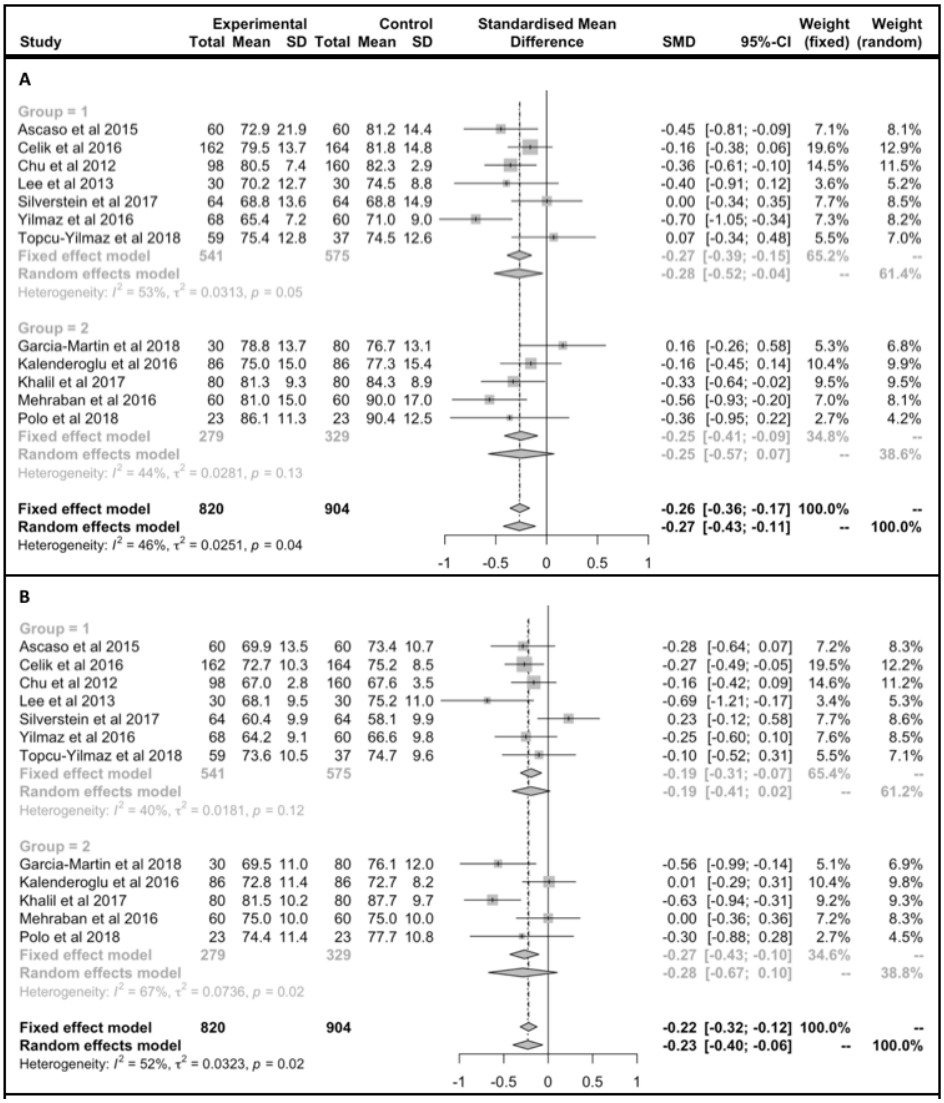

Figure 6. Meta-analysis data for (A) nasal and (B) temporal RNFL. Forest plots with fixed and random effects as well as SMD are given for RNFL data in probands, SZ (group 1) and BD (group 2). "Total" indicates the number of eyes whose measures are used to calculate mean difference. Horizontal bars in the forest plot indicate the 95% CI. Size of the square indicates the weight for each study.

Seven studies were included for analysis of the superior and inferior peripapillary RNFL, comprising of 460 patient eyes (320 SZ and 140 BD) and 514 HC eyes (374 from SZ and 140 from BD studies). In the superior RNFL, a significant decrease in thickness was seen in proband eyes compared to HC (SMD = -0.41, CI = -0.77 to -0.06, p = 0.03), but after adjusting

for publication bias, this effect was lost (Figure 7A, Appendix Figure 1D). Significant reductions were seen in BD eyes (SMD = -0.59, CI =-0.83 to -0.35) but not in SZ eyes (SMD = -0.34, CI = -0.88 to 0.20, Figure 7A). For the inferior RNFL, a trending reduction in thickness was found in proband eyes compared to HC (SMD = -0.33, CI = -0.69 to 0.03, p =0.065), but the results were lost after adjustment for publication bias (SMD = -0.059, CI = -0.45 to 0.33, p = 0.74, Figure 7B, Appendix Figure 1E). Similar to the superior RNFL, significant thinning was observed in BD eyes (SMD = -0.67, CI = -0.91 to -0.43) but not in SZ eyes (SMD = -0.18, CI = -0.63 to 0.28, Figure 7B).

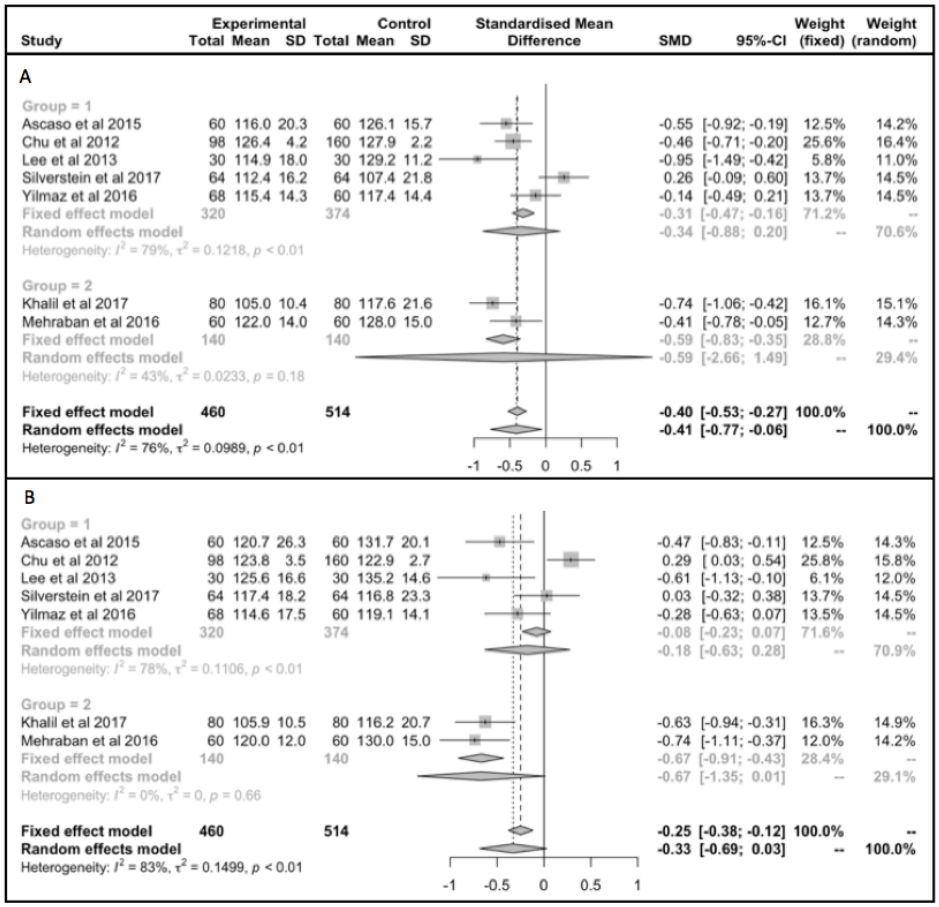

Figure 7. Meta-analysis data for (A) superior and (B) inferior RNFL. Forest plots with fixed and random effects as well as SMD are given for RNFL data in probands, SZ (group 1) and BD (group 2).

"Total" indicates the number of eyes whose measures are used to calculate mean difference. Horizontal bars in the forest plot indicate the 95% CI. Size of the square indicates the weight for each study.

Differences in GCL-IPL, GCC, and GCL

Four of the twelve studies reported a combined GCL-IPL measure, with a total of 329 eyes from probands (226 SZ and 103 BD) and 331 eyes from HC (228 from SZ and 103 from BD studies). One study, Celik et al 2016, provided separate GCL and IPL volume measurements, which were combined to provide a "GCL-IPL" value. Khalil et al 2017 gave the ganglion cell complex (GCC) measurement; this value was separated from the RNFL measurement given to calculate a "GCL-IPL" value. A significant reduction in GCL-IPL volume was observed between probands and HC (SMD = -0.39, CI = -0.55 to -0.24, $p < 0.001$), SZ and HC (SMD= -0.44, CI = -0.63 to -0.26) and BD and HC (SMD = -0.28, CI = -0.56 to -0.01, Figure 8A). The funnel plot indicated slight publication bias, and after adjustment via the trim and fill method, the results remained significant (SMD = -0.44, CI = -0.58 to =0.31, $p < 0.001$) (Appendix Figure 2A). Meta-regression analyses co-varying for age, sex, OCT device, and NOS score reported no relation to GCL-IPL volume (Appendix Table 1). Other factors, such as disease duration, severity of psychosis, smoking status, and antipsychotic dosage, were not analyzed due to too small of a sample size.

For the GCC, two studies were analyzed with a total of 103 BD eyes and 103 HC eyes. Significant thinning was seen (SMD = -0.94, CI = -1.23 to -0.65, $p < 0.001$, Figure 8B), and no publication bias was qualitatively seen in the funnel plot (Appendix Figure 2B).

Two studies (one SZ and one BD) were included for analysis of GCL volume for a total sample of 248 eyes from probands (162 SZ and 86 BD) and 250 eyes from HC (164 from SZ and 86 from BD studies). No significant reduction in GCL volume was observed

between probands and HC (SMD = -1.83, CI = -9.53, 5.88, p = 0.20, Figure 8C). In SZ and BD, reductions in volume were seen, but because of the high levels of heterogeneity between the two studies, no overall significance was reported. The funnel plot indicated publication bias, but there were not enough samples to perform trim and fill method analysis (Appendix Figure 2C).

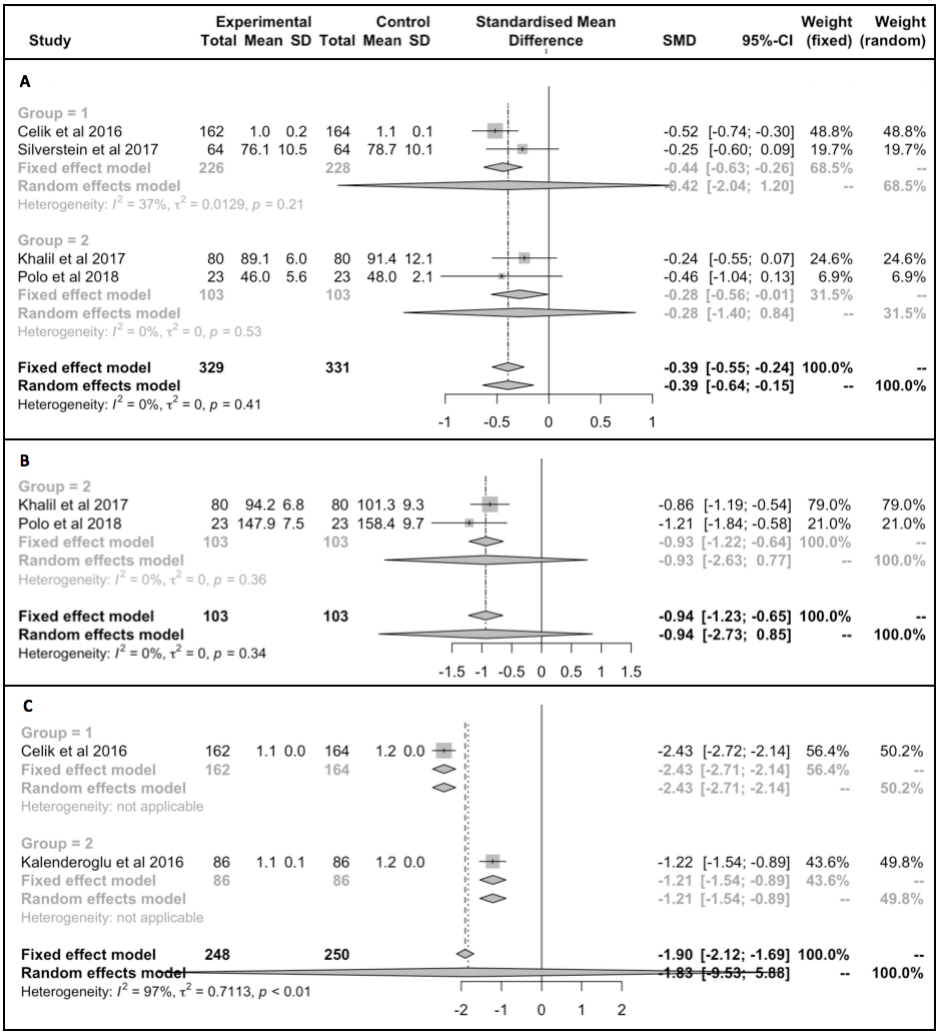

Figure 8: Meta-analysis data for (A) GCL-IPL, (B) GCC, and (C) GCL. Forest plots with fixed and random effects as well as SMD are given for RNFL data in probands, SZ (group 1) and BD (group 2). "Total" indicates the number of eyes whose measures are used to calculate mean difference. Horizontal bars in the forest plot indicate the 95% CI. Size of the square indicates the weight for each study.

Differences in Choroidal Thickness

Four studies, with a total of 330 eyes from probands (221 SZ and 109 BD eyes) and 310 eyes from HC (201 from SZ and 109 from BD studies), were analyzed to study average choroidal thickness (CT). No differences were seen between probands and HC (SMD = -0.01, CI = -0.43 to 0.42, p = 0.96, Figure 9A). Furthermore, no significant thinning was found in SZ eyes (SMD = -0.09, CI = - 2.31 to 2.73) and in BD eyes (SMD = -0.16, CI = 0.10 to 0.43, Figure 9A). Qualitative assessment indicated publication bias, and after adjustment, no significant differences arose between probands and controls (SMD = -0.25, CI = -0.71 to 0.20, p =0.21, Appendix Figure 3).

Differences in Macular Thickness and Volume

For macular thickness (MT), four studies (3 SZ and 1BD) were included for a total of 185 eyes from probands (162 SZ and 23 BD) and 177 eyes from HC (154 from SZ and 23 from BD studies). No significant reductions in thickness were seen (SMD = -0.61, CI = 1.46 to 0.25, p 0.11, Figure 9B). After adjustment for publication bias, no significant results arose (SMD = -0.27, CI = -1.05 to 0.50, p = 0.40, Figure 9B).

Four SZ studies, with a total of 252 SZ eyes and 314 HC eyes, were analyzed for macular volume (MV) measures. No significant decreases in MV were observed (SMD = -0.46, CI = -1.60 to 0.69, p = 0.29, Figure 9C). Quantitative adjustment for publication bias via the trim and fill method reported a significant reduction in MV between SZ and HC (SMD = -0.20, CI = -0.37 to -0.03, p = 0.023, Appendix Figure 3C).

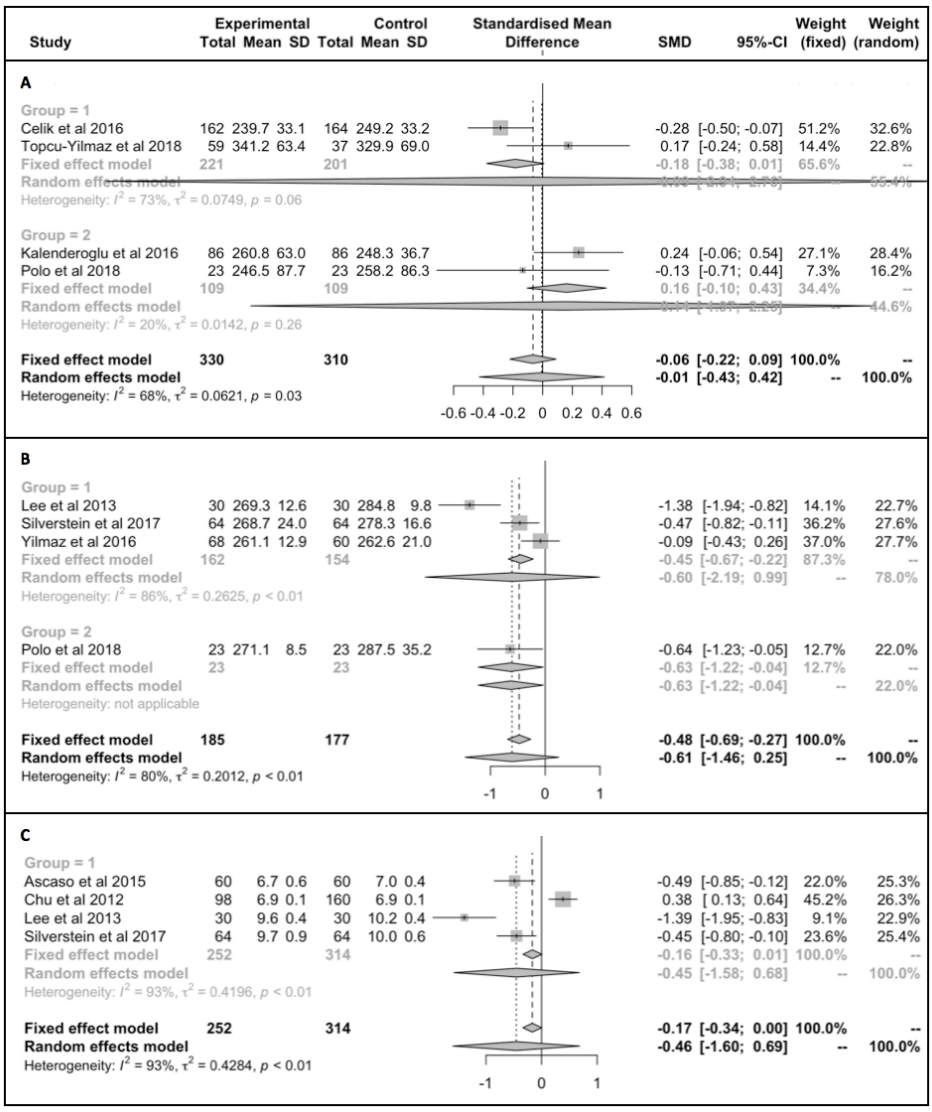

Figure 9: Meta-analysis data for (A) CT, (B) MT, and (C) MV. Forest plots with fixed and random effects as well as SMD are given for RNFL data in probands, SZ (group 1) and BD (group 2). "Total" indicates the number of eyes whose measures are used to calculate mean difference. Horizontal bars in the forest plot indicate the 95% CI. Size of the square indicates the weight for each study.

Out of all regions, the overall peripapillary RNFL, superior RNFL, and GCL-IPL displayed the largest effect sizes between probands and (Figure 10). Smaller but still significant effects were seen for the nasal and temporal RNFL. It should be noted that all groups (probands,

SZ, and BD) showed significant reductions for the overall and nasal RNFL as well as the GCL-IPL.

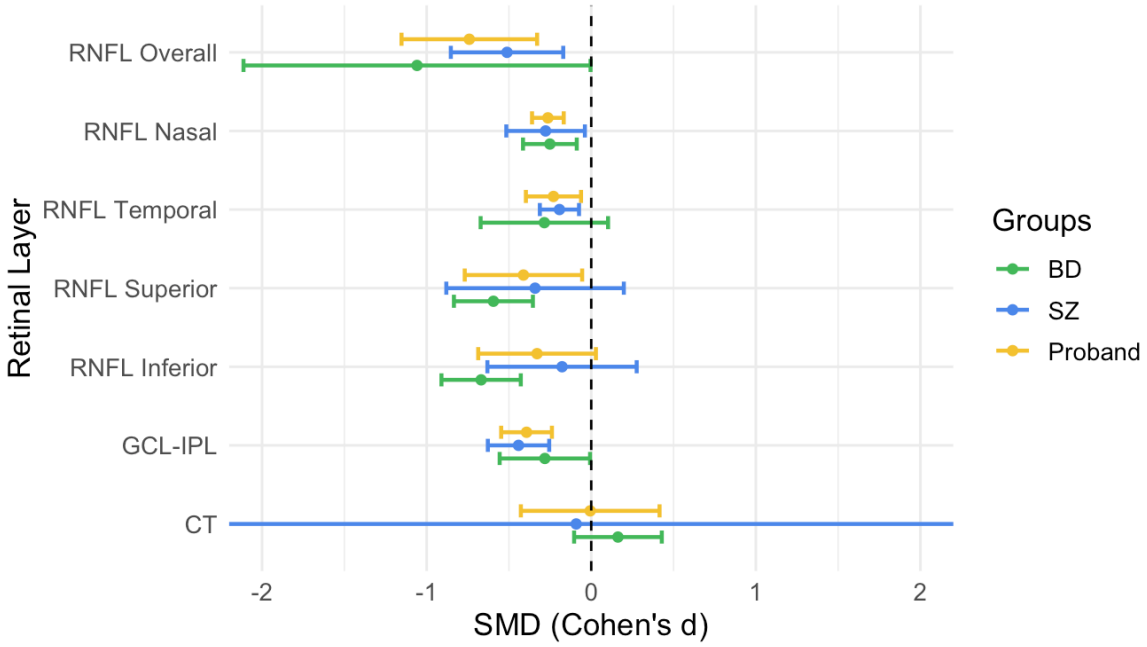

Figure 10: Forest plot of significant retinal segments and effect size. Circles represent the SMD effect size (Cohen's d), with the horizontal bars indicating the 95% CI. Groups indicate probands (overall, SZ, and BD) compared to HC eyes.

Pilot Study Analysis

The demographic data for the 38 participants is listed in Table 2. The diagnostic groups showed no significant differences due to sex, race, and age (T = 2.96, p = 0.40; T= 7.89, p = 0.25; T= 1.33, p = 0.28). No significant group differences were seen for right VA, left VA, or overall VA (T = 3.42, p = 0.33; T = 6.74, p = 0.35; T= 1.94, p = 0.14). Trending differences were observed for the average BMI between groups (T = 2.81, p = 0.054).

Table 2: Demographics data.

Variable	BD	HC	SAD	SZ	T Statistic	p
Sex (Female/Male)	4/2	6/8	2/5	3/8	2.96	0.40
Race (AA/CA/OT)	0/5/1	4/9/1	1/5/1	5/3/3	7.89	0.25
Visual Correction (Corrected/Uncorrected)	4/2	6/8	4/3	6/5	1.08	0.78
Right Visual Acuity (Mild/Normal)	2/4	6/5	5/1	4/5	3.42	0.33
Left Visual Acuity (Mild/Moderate/Normal)	2/0/3	5/0/7	4/0/2	3/2/4	6.74	0.35
Mean Age	29.8 (11.1)	39.4 (13.0)	32.6 (11.7)	40.5 (14.1)	1.33	0.28
Mean BMI	26.6 (6.8)	26.2 (4.2)	28.1 (3.6)	32.0 (6.4)	2.81	0.054
Mean Visual Acuity	0.91 (0.21)	0.94 (0.24)	0.66 (0.23)	0.86 (0.33)	1.94	0.14
Mean Chlorpromazine Dose	66.3 (NA)	-	406.0 (352.7)	239.4 (NA)	0.428	0.68

Note: Data are presented as mean (standard deviation). AA, African American; CA, Caucasian; OT, Other; BMI, body mass index; SAD, Schizoaffective disorder.

OCT Data

Group differences analysis studied via multivariate comparisons for retinal layer data in right (OD), left (OS), and mean (OD and OS averaged) measurements. Covariates included age, sex, race, BCVA and BMI. For OD analyses, the right VA was used as a covariate, and for OS analyses, the left VA was used.

Mean Eye Group Differences

In mean eye analyses, no significant group differences were seen for the overall retinal thickness. The overall RNFL displayed trending thinning in probands compared to HC ($t = -1.72$, $p = 0.095$), and the overall and outer OPL showed trending thickening ($t = 1.98$, $p = 0.057$; $t = 2.04$, $p = 0.051$, Figure 11A, Appendix Table 3). Similarly, the SZ diagnostic group demonstrated a trending reduction in the overall RNFL ($t = -1.99$, $p = 0.058$) and increases in overall, inner, and outer OPL thickness ($t = 2.82$, $p = 0.009$; $t = 2.18$, $p = 0.040$; $t = 2.87$, p

= 0.008, Figure 11B, Appendix Table 3). The BD group showed a trending decrease in central RNFL thickness (t = -2.08, p = 0.060, Figure 11C, Appendix Table 3).

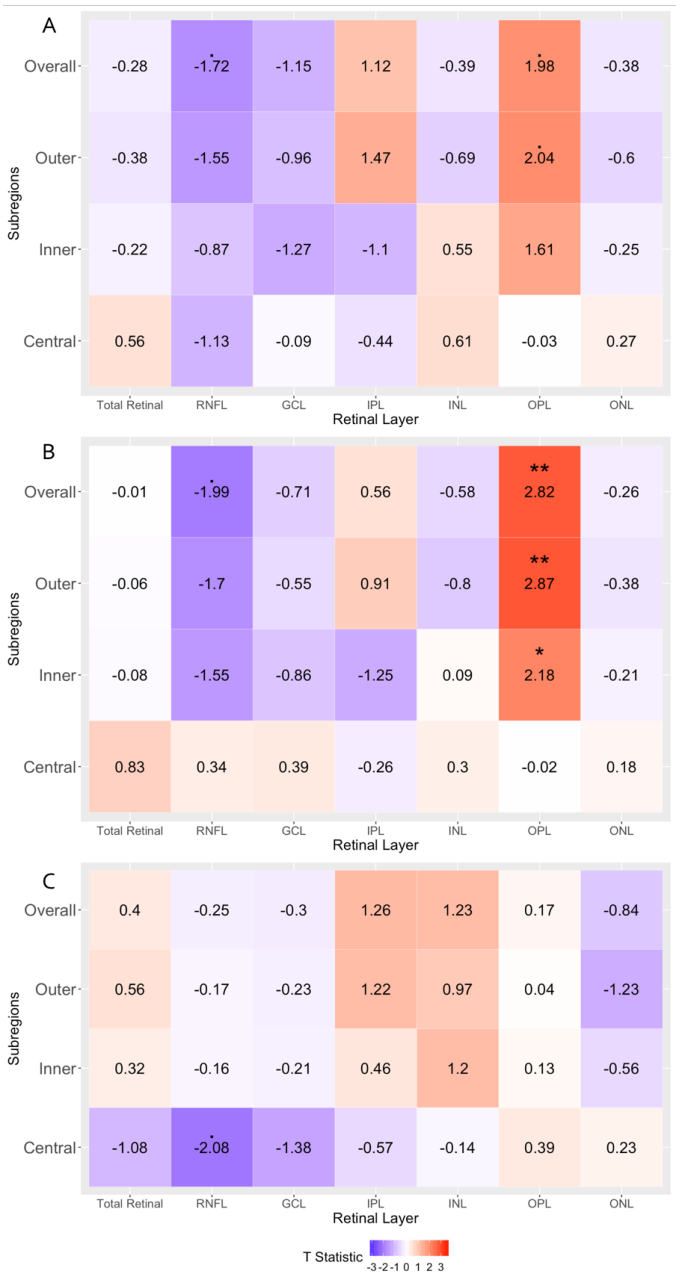

Figure 11: T-stat heat map of mean retinal layer differences. Sub-maps are for (A) probands vs. HC, (B) SZ vs. HC, and (C) BD vs. HC. Darker red color indicates higher thickness in probands compared to controls, while a darker blue color indicates lower thickness. Statistically significant results are indicated with: (a) '-' for $p < 0.1$, (b) '*' for $p < 0.05$, (c) '**' for $p < 0.01$, and (d) '***' for $p < 0.001$.

Right Eye Group Differences

No significant changes in retinal layers were seen in proband and SZ groups compared to HC for right eye retinal measures (Figures 12A and 12B). In the BD group, the central RNFL displayed a trending decrease in ($t = -1.95$, $p = 0.075$, Figure 11C, Appendix Table 4).

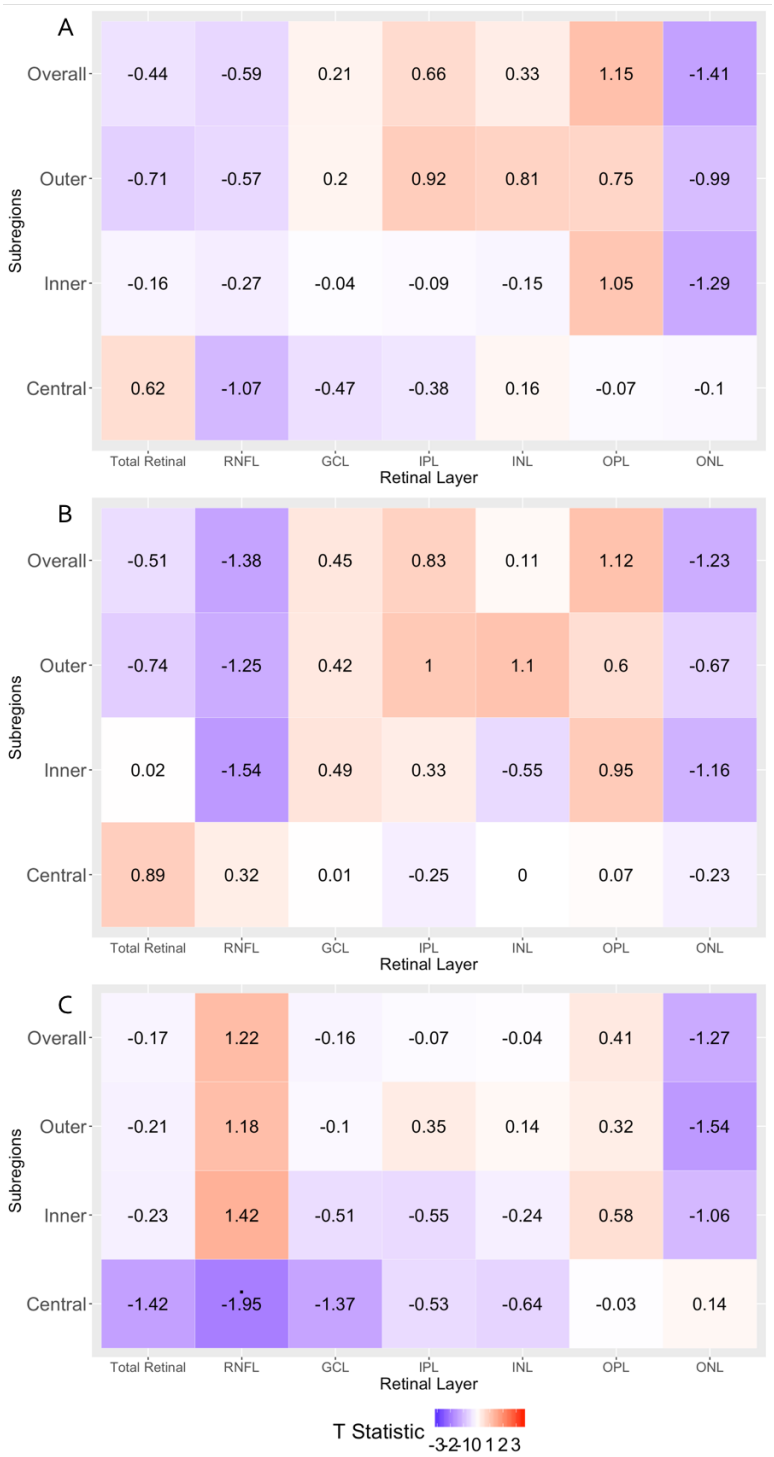

Figure 12. T-stat heat map of right eye retinal layer differences in (A) probands vs. HC, (B) SZ vs. HC, and (C) BD vs. HC. Darker red color indicates higher thickness in probands compared to controls, while a darker blue color indicates lower thickness. Statistically significant results are indicated with: (a) '-' for $p < 0.1$, (b) '*' for $p < 0.05$, (c) '**' for $p < 0.01$, and (d) '***' for $p < 0.01$.

Left Eye Group Differences

For probands, the left eye showed significant thickening of the overall, inner, and outer OPL ($t = 2.08$, $p = 0.046$) and a trending thinning of the inner and outer ONL ($t = -1.8$, $p = 0.082$, Figure 13A, Appendix Table 4). In SZ eyes, there were increases in overall, inner, and outer OPL thickness ($t = 2.56$, $p = 0.017$; $t = 2.57$, $p = 0.017$; $t = 2.57$, $p = 0.017$, Figure 13B, Appendix Table 5) as well as trending reductions in the overall, inner, and outer ONL ($t = -1.88$, $p = 0.072$; $t = -2.03$, $p = 0.054$; $t = -2.03$, $p = 0.054$, Figure 13B, Appendix Table 5). BD eyes displayed trending increases in inner and outer RNFL ($t = 2.02$, p 0.065) and trending reductions in the central RNFL ($t = -2.03$, $p = 0.065$, Figure 13C, Appendix Table 5).

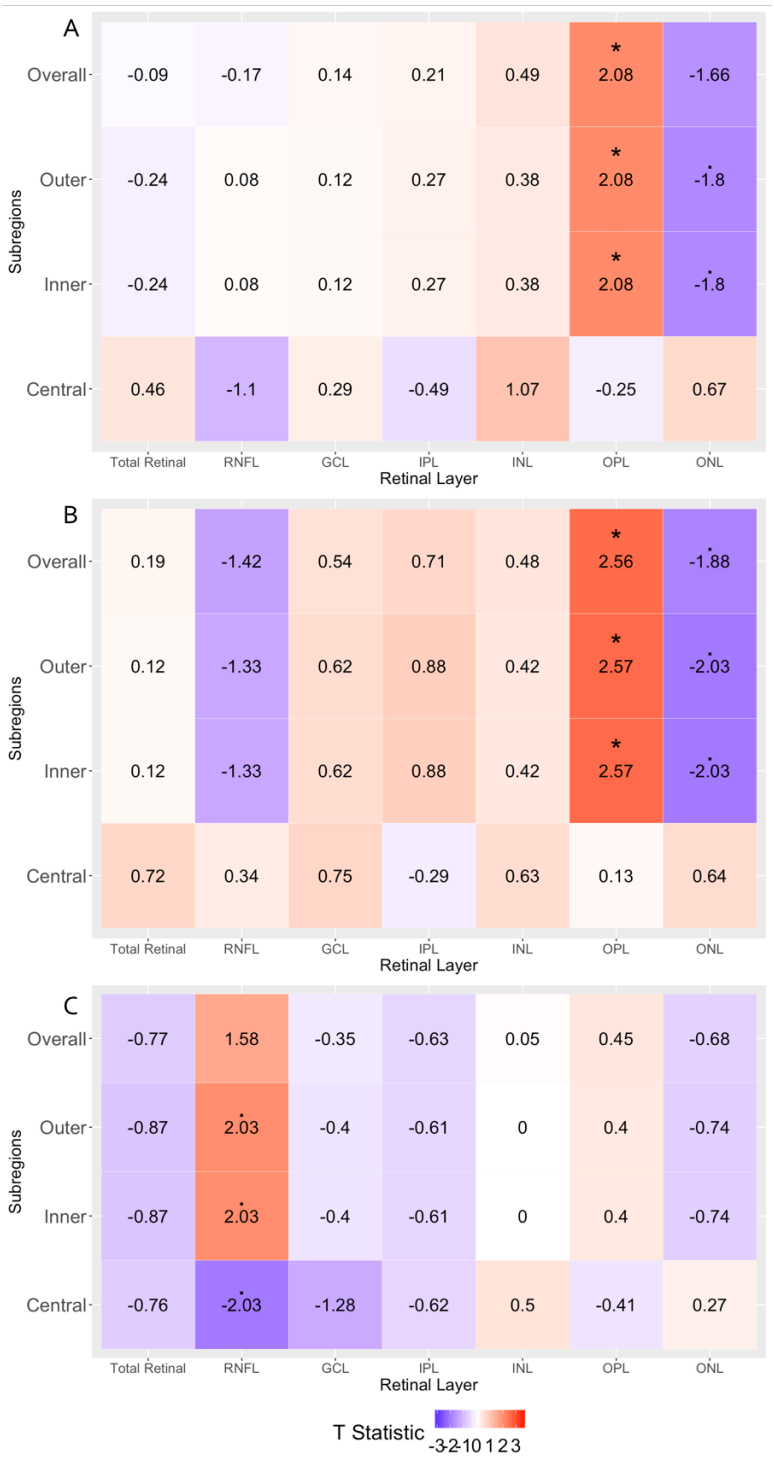

Figure 13. T-stat heat map of left eye retinal layer differences. in (A) probands vs. HC, (B) SZ vs. HC, and (C) BD vs. HC. Darker red color indicates higher thickness in probands compared to controls, while a darker blue color indicates lower thickness. Statistically significant results are indicated with: (a) '-' for $p < 0.1$, (b) '*' for $p < 0.05$, (c) '**' for $p < 0.01$, and (d) '***' for $p < 0.01$.

Clinical Correlations

Clinical measures such as illness duration, PANSS total and positive/negative symptom total scores, antipsychotic dosage, and smoking status were analyzed for correlation to retinal layer thickness. Covariates of age, sex, race, BMI, and VAC were used in all analyses, with the exception of antipsychotic dosage due to small sample size.

Illness duration, PANSS score, and PANSS positive subscore did not show any significant correlations to retinal layer thickness (Figures 14 A-C). PANSS negative total score demonstrated a significant negative correlation with overall GCL thickness ($t = -2.33$, $p = 0.048$) as well as trending negative relationships with the central RNFL, inner GCL, and outer GCL ($t = -1.90$, $p = 0.09$; $t = =1.92$, $p = 0.091$; $t = -1.91$, $p = 0.09$, Figure 14D, Appendix Table 8). Average chlorpromazine dosage showed a trending positive correlation to overall retinal thickness ($t = 2.42$, $p = 0.06$). In addition, there was an inverse relationship between antipsychotic dosage and overall and outer IPL ($t = -2.27$, $p = 0.072$; $t = -2.28$, $p = 0.071$, Figure 14E, Appendix Table 10). Finally, no correlations were observed between retinal measures and smoking status (Figure 14F).

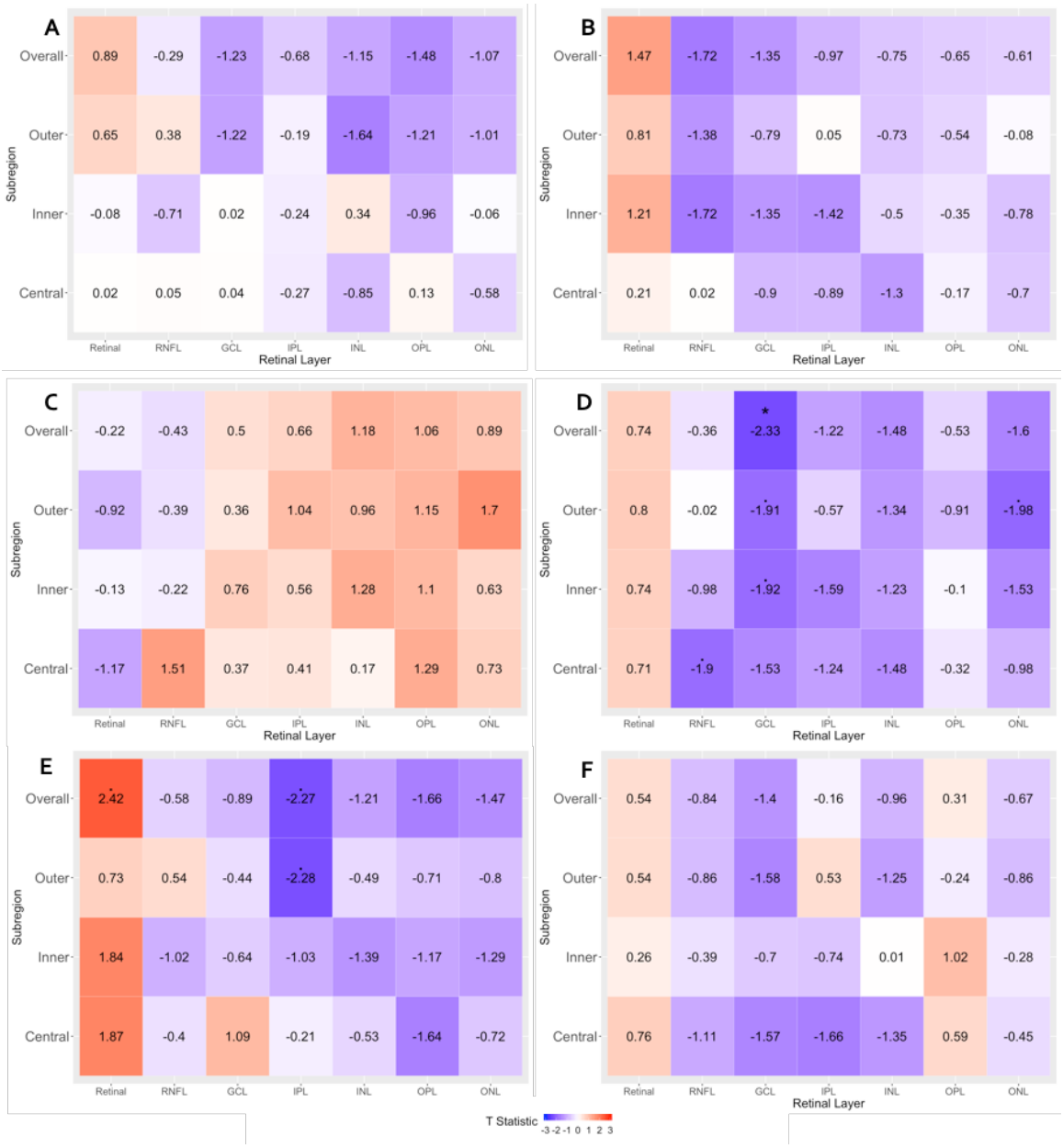

Figure 14. Clinical association t-stat heat map. Clinical measures include (A) illness duration, (B) PANSS total score, (C) PANSS positive symptom score, (D) PANSS negative symptom score, (E) average chlorpromazine dosage, and (F) smoking status. Darker red color indicates higher thickness in probands compared to controls, while a darker blue color indicates lower thickness. Statistically significant results are indicated with: (a) '-' for $p < 0.1$, (b) '*' for $p < 0.05$, (c) '**' for $p < 0.01$, and (d) '***' for $p < 0.01$.

Structural MRI Correlations

Total gray matter thickness, gray matter volume, and intracranial volume were analyzed for correlations to retinal layer thickness. Figure 15 illustrates correlation heat maps of the t statistics for mean retinal layer and cortical measures. A trending positive relationship was observed between ICV and the outer total retinal thickness ($t = 1.92$, $p = 0.07$, Figure 15A**,** Appendix Table 12). A significant inverse relationship was found between total GM thickness and inner RNFL ($t = -2.17$, $p = 0.04$, Figure 15B**,** Appendix Table 12). The outer GCL displayed a slight slight trending negative relationship with ICV ($t = -1.76$, $p = 0.09$, Figure 15C, Appendix Table 12). No correlations were seen between the cortical measures and IPL or the INL (Figures 15D and 15E, Appendix Table 12). The inner and overall regions of the OPL showed a significant and trending negative correlation with ICV, respectively ($t = -2.72$, $p = 0.01$; $t = -1.83$, $p = 0.08$). In addition, the inner OPL and GM volume had a trending negative correlation ($t = -1.79$, $p = 0.088$, Figure 14F, Appendix Table 12). Lastly, the central ONL showed a trending negative correlation with the total GM thickness ($t = -1.95$, $p = 0.066$, Figure 15G, Appendix Table 12).

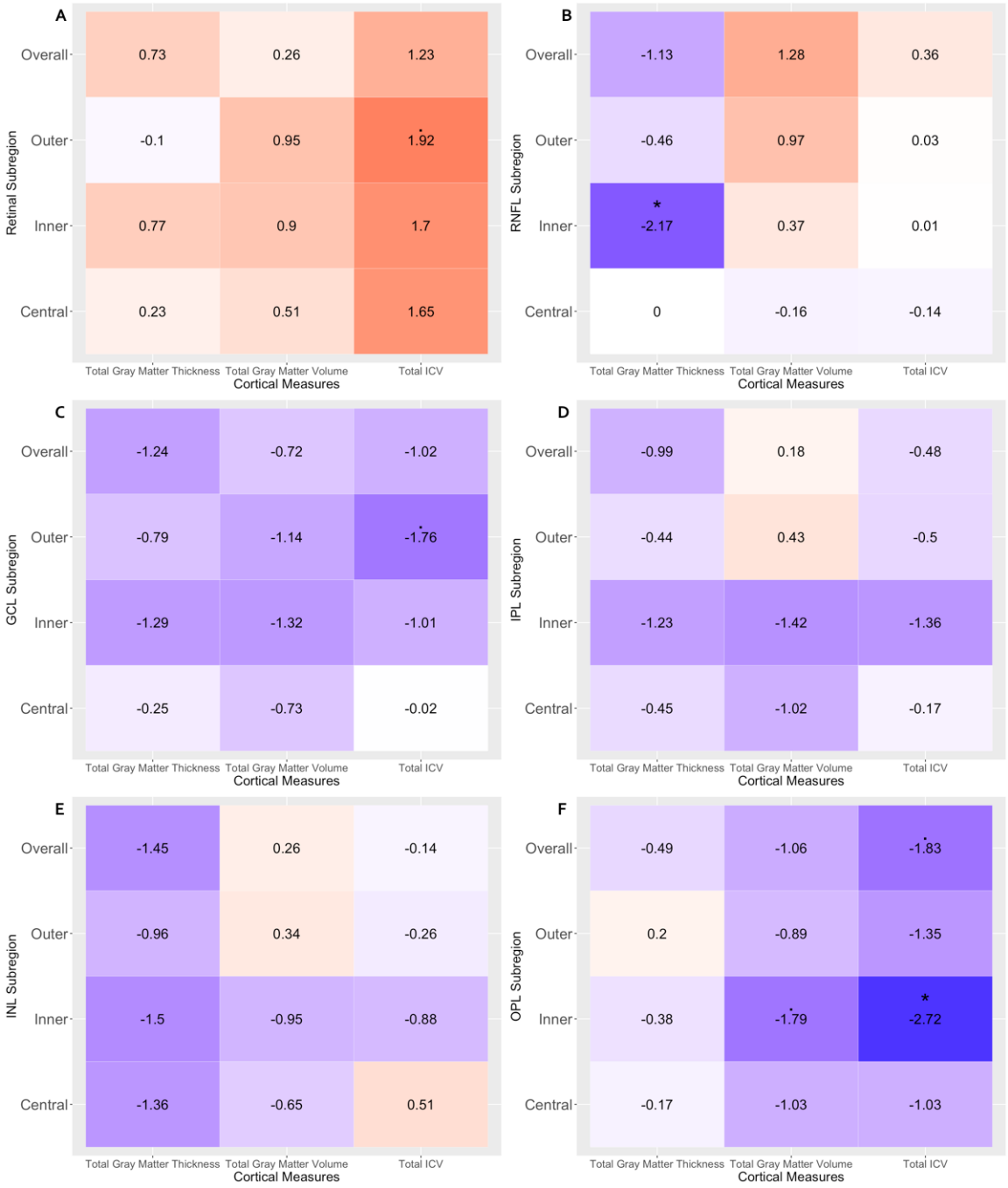
A
Retinal Subregion
Overall
Outer
Inner
Central
0.73
0.26
1.23
-0.1
0.95
1.92
0.77
0.9
1.7
0.23
0.51
1.65
Total Gray Matter Thickness
Total Gray Matter Volume
Total ICV
Cortical Measures
B
RNFL Subregion
-1.13
1.28
0.36
-0.46
0.97
0.03
*
-2.17
0.37
0.01
0
-0.16
-0.14
C
GCL Subregion
-1.24
-0.72
-1.02
-0.79
-1.14
-1.76
-1.29
-1.32
-1.01
-0.25
-0.73
-0.02
D
IPL Subregion
-0.99
0.18
-0.48
-0.44
0.43
-0.5
-1.23
-1.42
-1.36
-0.45
-1.02
-0.17
E
INL Subregion
-1.45
0.26
-0.14
-0.96
0.34
-0.26
-1.5
-0.95
-0.88
-1.36
-0.65
0.51
F
OPL Subregion
-0.49
-1.06
-1.83
0.2
-0.89
-1.35
-0.38
-1.79
*
-2.72
-0.17
-1.03
-1.03

Figure 15. Cortical-retinal structure association t-stat heat map. Sub-figures represent heatmaps for (A)Total retina, (B) RNFL, (C) GCL, (D) IPL, (E) INL, (F) OPL, (G) ONL. Darker red color indicates higher thickness in probands compared to controls, while a darker blue color indicates lower thickness. Statistically significant results are indicated with: (a) '-' for $p < 0.1$, (b) '*' for $p < 0.05$, (c) '**' for $p < 0.01$, and (d) '***' for $p < 0.01$.

DISCUSSION

Meta-Analysis Findings

Disclaimer: This section has been adapted from the author's co-first author publication: Lizano, P., Bannai, D., Lutz, O., Kim, L. A., Miller, J., & Keshavan, M. (2020). A Meta-analysis of Retinal Cytoarchitectural Abnormalities in Schizophrenia and Bipolar Disorder. *Schizophrenia Bulletin*, *46*(1), 43–53. https://doi.org/10.1093/schbul/sbz029. Overall, the meta-analysis established that compared to HC, there is significant atrophy in the overall and nasal RNFL related to psychosis. Significant thinning of the temporal RNFL was found in the proband and SZ group, while reductions in superior and inferior RNFL were only seen in BD eyes. In addition, significant reductions of the GCL-IPL were observed across proband, SZ, and BD groups, while GCC thinning was only seen in BD. No differences were found for the GCL. In addition, MT and CT measures showed no differences between groups. Finally, significant reductions in MV were found for the SZ group. All findings were cross-validated and controlled and adjusted for publication bias. Furthermore, meta-regression analysis into age, sex, disease duration, OCT device and NOS score were found to be unrelated to RNFL, GCL-IPL, or choroidal thickness.

The RNFL findings are of significant interest since it contains unmyelinated ganglion cell axons that parallel to the surface of the retina and converge to form the optic nerve. These fibers project mainly to the LGN of the thalamus and therefore are the main sensory input to the visual cortex (Mancall & Gray, 2011). Damage can occur at any point in the visual pathway resulting in atrophy of ganglion cells and their axons (GCL and RNFL, respectively) in a retrograde process (Petzold et al., 2016). The concept of retrograde trans-

synaptic degeneration (RTSD) has been well documented in animal models, where destruction of the occipital lobe was associated with decreases in thalamic LGN cells, thus leading to decreases in retinal ganglion cell density (Dinkin, 2017). In human models, a study by Gabilondo et al. (2014) supported the presence of RTSD in the posterior visual pathway in patients with MS, a disease characterized by chronic axonal degeneration.

The thalamus plays an important role in the pathophysiology of SZ and BD. It is the central relay center between sensory information and cortical regions such as the cerebral cortex and cerebellum, that control various cognitive functions (Dorph-Petersen & Lewis, 2017). Literature shows that the thalamus is largely affected in SZ and BD through alterations in volume, structural connectivity, activation, and cell number (Cho et al., 2019; Dorph-Petersen & Lewis, 2017; Ng et al., 2009). It can be hypothesized that inflammatory or oxidative stress pathways in addition to aberrations in microvasculature may lead to RTSD and retinal layer atrophy, but no studies have tested this in SZ or BD.

RNFL

The overall and superior RNFL showed the largest effect size differences in thickness between probands and HC. The nasal and superior RNFL showed significant thinning in both SZ and BD groups. Five articles showed significant reductions in RNFL thickness due to illness duration (Chu et al., 2012; Kalenderoglu et al., 2016; Lee et al., 2013; Mehraban et al., 2016; Polo et al., 2018). However, six articles showed no relationship (Ascaso et al., 2015; Celik et al., 2016; Garcia-Martin et al., 2018; Khalil et al., 2017; Steven M. Silverstein et al., 2017; Topcu-Yilmaz et al., 2018). The sample from articles containing RNFL measures had mixed chronic and acute disease states. While the meta-regression showed no effects of

illness duration on RNFL thickness, a separate analysis into acute vs. chronic states could not be done because half of the studies combined these two groups. Symptom severity was sparsely reported and not analyzed for meta-regression. Kalenderoglu et al. (2016) found an association between RNFL thinning and symptom severity, while the other 11 articles found no such relationship. Ascaso et al. (2015) proposed that neuro-inflammation in acute psychotic states may increase RNFL thickness and thus mask the decreases seen in chronic patients. Age, sex, and OCT device were confounders that did not have any correlation with RNFL thickness. However, reductions in RNFL thickness with age have been well documented (Demirkaya et al., 2013). Variables that have been shown to be cofounders but not tested due to small sample size included medication (dosage), smoking, and cardio-metabolic disease. Silverstein et al. (2017) demonstrated that the presence of diabetes and hypertension was associated with a significant reduction in RNFL thickness. This association has been seen in previous studies (Garcia-Martin et al., 2017; Zarei et al., 2017). Silverstein et al. (2017) did not see any significant correlation between antipsychotic dosage and RNFL thickness, and Mehraban et al. (2016) did not demonstrate any effects from smoking.

GCL-IPL, GCC, and GCL

The GCL rests below the RNFL and is comprised of ganglion cell bodies, astrocytes, and amacrine cells. Advances in OCT technology from first generation TD-OCT to second and third generation SD- and SS-OCT have allowed for better segmentation of the GCL. The IPL contains the synapses of the dendrites of the ganglion cells and the axons of the bipolar and amacrine cells. The ganglion cell processes project to the LGN of the thalamus, and therefore, decreases in GCL and IPL thickness may reflect neuronal or synaptic atrophy.

Saidha et al. (2013) proposed that the GCL and IPL are better markers of disease severity in MS compared to the RNFL, likely due to the fact that the RNFL is sensitive to inflammatory effects. The results of the meta-analysis demonstrate a reduction in GCC and GCL-IPL, suggesting that the two layers are involved in the pathophysiology of SZ and BD. Because the sample size of these analyses contained four or fewer articles, further studies are required to determine which layer is most affected and to what degree.

No significant relationships between each of these three regions and age, sex, and OCT device were seen. Other clinical measures were not able to be analyzed with meta-regressions due to a small sample size. One study observed correlations between lower GCL and IPL volumes and illness duration and symptom severity (Celik et al., 2016). Garcia-Martin et al. (2018), however, found a significant positive correlation between GCL volume volume and illness duration, while Khalil et al. (2017) found no associations between GCC thickness and illness duration or symptom severity. Another study showed that the average GCL-IPL thickness was decreased in patients with cardio-metabolic issues (hypertension or diabetes) but no conclusive relationship could be established due to small sample size (Silverstein et al., 2017). With regards to smoking, no articles found differences in GCL volume (Kalenderoglu et al., 2016). While further studies are warranted, it can be hypothesized that neuronal and synaptic loss, strongly linked to the pathophysiology of SZ and BD, are related to the reductions seen in the GCL and IPL (Dorph-Petersen & Lewis, 2017).

Choroid

The choroid contains a complex vascular bed and supplies the outer retinal layers with nutrients, in addition to maintaining the temperature and volume of the eye (Mancall & Gray, 2011). The choroid also houses immunoreactive cells (Ehrlich et al., 2010). No significant findings were seen in CT from the meta-analysis between probands and HC. Celik et al. (2016) found significant reductions in CT in treatment refractory probands compared to those who were treatment responsive. Furthermore, they found that CT was negatively correlated with symptom severity. However, Topcu-Yilmaz et al. (2018) reported a slight correlation between CT and illness duration. Because the findings are mixed, further studies are required to clarify the role of CT in SZ and BD.

Macula

Very few studies included macular volume or thickness, and no studies included macular segmentation. After adjustment for publication bias, significant reductions in MV were seen in probands compared to HC. No significant correlations were seen for illness duration, symptom severity, or any other clinical measure (Ascaso et al., 2015; Chu et al., 2012). Because of the small sample size (n=2) for these analyses, further investigation is necessary to better understand the role of the macula in SZ and BD.

Limitations

This meta-analysis has several limitations associated. First, the total number of studies (n=12) is small, and the data from these papers varied in the retinal segmentation measures reported. For example, reporting of the GCL-IPL measure was variable, so the GCL, IPL, and GCL-IPL data was pooled in order to increase statistical power. Some studies included

right and left eye data, which was pooled for a mean value, while other studies reported data from one eye. Other limitations included heterogeneity in the studies included, variability in OCT device used, and publication bias. These were addressed in the meta-analysis by utilizing random effects models when necessary, performing cross-validation analysis, adjusting for publication bias via the trim and fill method, and conducting a meta-regression analysis for OCT device.

Pilot Study Findings

The results of the meta-analysis gave information on which regions to specifically look at in the preliminary analysis, namely the RNFL and GCL-IPL. In addition, it provided a comprehensive review of the current literature relating to retinal imaging in psychosis. However, the papers in the meta-analysis only provided measures for three of eight layers (RNFL, GCL, and IPL) in addition to CT. Only a few analyzed relevant clinical measures such as smoking status, illness duration, and antipsychotic dosage. There was also variation in the data measures presented in each article, where some reported averaged right and left eye measures and others reported only right or left eye measures as representative for both eyes. Lastly, no articles analyzed correlations between neuroimaging and retinal layer measures. The pilot study was aimed to replicate previous findings and to fill in informational gaps present in literature.

Overall, the preliminary found trending reductions in the RNFL, increases in the OPL, and reductions in the ONL. No changes in thickness were seen for the GCL, IPL, or INL. For the clinical measures, the PANSS negative total score showed a negative relationship with GCL thickness, and antipsychotic dosages demonstrated a negative

relationship with IPL thickness. Finally, for neuroimaging measures, negative correlations were observed between the gray matter thickness and RNFL and ONL thickness, and the OPL saw a negative relationship with total ICV.

Overall Retina

The total retinal thickness showed no significant differences between proband SZ, and BD eyes compared to healthy controls in mean, right, and left eye measurements.

Antipsychotic dosage demonstrated a trending positive correlation with overall retinal thickness, with a general trend seen across the central, inner, and outer regions. Medication has been shown to have an anti-inflammatory in SZ (Li & Xu, 2007), and this neuro-protective effect could be what is seen from the positive correlation with the overall retinal thickness. PANSS total score and positive symptom score showed a positive trend with retinal layer thickness. PANSS negative score displayed a negative relationship between retinal layer thickness. This finding is consistent with associations seen between thinning of the prefrontal cortex and negative symptom severity in SZ (Walton et al., 2018). Moreover, it supports the RTSD hypothesis linking reductions in cortical measures to reductions in retinal layer thickness.

A trending positive correlation was observed between the outer retinal thickness and total ICV. All sub-regions of total retinal thickness demonstrated a positive trend with GM thickness, GM volume, and total ICV. This is expected, as retinal thickness would correlate to GM integrity.

RNFL

Overall, slight trending reductions were seen in the overall RNFL in probands and SZ eyes compared to HC eyes. No significant differences in any region of the RNFL were seen in the right eye, while the left eye showed trending increases in the inner and outer RNFL reductions in the central RNFL. These results are consistent with the meta-analysis and literature showing RNFL atrophy in psychosis.

The increase in thickness observed in the left eye may be explained by a neuro-inflammatory response. The role of neuro-inflammation in the pathophysiology of psychotic disorders has recently been well-studied. Aricioglu et. al (2016) demonstrated that various inflammatory marker increases are associated with SZ, including increases in peripheral cytokine levels (namely, interleukin-6, tumor necrosis factor α, and C-reactive protein), hyperactivation and damaged functionality of astrocytes, and disturbances in monocytic immune responses. In bipolar disorder, similar elevations in peripheral cytokine levels and glial dysfunctions have been observed (Muneer, 2016). These disruptions can alter the permeability of the blood brain barrier (BBB), causing disruption and leading to changes in the retinal layer measurements.

Clinical measures such as illness duration, PANSS total score, PANSS positive symptom score, antipsychotic medication dosage, and smoking status showed no relationship to RNFL thickness. Past studies have shown similar results (Mehraban et al., 2016; Silverstein & Keane, 2011). A trending inverse relationship between PANSS negative symptom score and central RNFL thickness was observed. Kalenderoglu et al. (2016) found a negative relationship between symptom severity and global RNFL thickness. However, their symptom measures included the Young Mania Rating Scale (YMRS) and Clinical Global Impression (CGI), not PANSS.

With regards to cortical measures, the inner RNFL showed a significant inverse correlation with total gray matter thickness. This result is contradictory to previous literature supporting a positive relationship between RNFL and GM thickness and could be due to the small sample size.

GCL and IPL

No significant differences were observed in the GCL and IPL in probands, SZ, or BD compared to HC for mean, left, and right eye values. This is inconsistent with the meta-analysis GCL-IPL reduction finding, even if GCL and IPL measures were not combined in the preliminary analysis.

The GCL showed a general negative relationship to duration of illness, PANSS negative score, antipsychotic dosage, and smoking but did display a positive relationship with PANSS positive score. Garcia-Martin et al. (2018) found a similar negative relationship between GCL thickness and disease duration. Celik et al. (2016) reported negative correlations between total PANSS score and illness duration to the right GCL.

The IPL demonstrated no correlation with illness duration, PANSS total score, PANSS positive score, PANSS negative score, and smoking status. A trending inverse relationship between the overall and outer IPL antipsychotic was observed. Celik et al. (2016) found a strong negative correlation between right IPL thickness and disease duration and total PANSS score and was the only study to report any IPL thickness relationship to clinical measures.

The overall GCL had a negative relationship with all three cortical measures, with the correlation between outer GCL and ICV being both negative and trending. Furthermore, the

IPL showed an overall negative relationship with GM thickness and volume and ICV. While not significant, these trends contradict the association of retinal and cortical integrity.

INL, OPL, and ONL

The INL, OPL, and ONL were not included in the meta-analysis because not enough articles collected and reported these measures. From the preliminary analysis, no significant thickness differences were found for the INL in probands, SZ, and BD compared to HC. Trending increases in the overall and outer OPL thickness was observed in probands and SZ eyes compared to HC eyes. Furthermore, the SZ group showed significant thickening of the inner OPL. Left eye overall, inner, and outer OPL measures were found to be significantly increased in probands. Right eye overall, inner, and outer OPL were observed in SZ. Samani et al. (2018) had similar but not significant findings that demonstrated increases in OPL thickness in SZ. In addition, thickening of the OPL has been observed in Parkinson's disease with the suggestion that foveal remodeling from oxidative stress pathways may explain the findings (Chorostecki et al., 2015; Pilat et al., 2016). Finally, the inner and outer ONL saw trending thinning in probands compared to HC, which is consistent with what was observed by Samani et al. (2018).

No significant correlations were found between all three layers and clinical measures. With regards to cortical measures, no correlations were determined with the INL. The OPL demonstrated a significant negative relationship with total ICV, while the ONL showed a trending negative relationship with total gray matter thickness. Samani et al. (2018) found an inverse relationship between ONL thickness and PANSS negative symptom score but did not report any cortical correlations between any of these three layers.

Few studies have reported on INL, OPL, and ONL thickness differences due to limitations in retinal segmentation resolution in older generation OCT devices. Now with SD- and SS-OCT, these layers are more easily and reliably parsed out. Further investigation into the changes in these layers is warranted, since these findings are novel in not only psychiatric disorders such as SZ or BD but also in neurologic disorders in general.

Limitations

One limitation for this exploratory analysis is a small sample size (n=38). Increasing the power for this study would greatly increase the confidence to which the results may be interpreted, and active recruitment is underway for this study. Further studies expanding the number of cortical measures analyzed would help to better test the RTSD hypothesis, especially in the thalamic region and its related structures.

Conclusion

In all, the use of OCT to study the underlying neurobiology of SZ and BD shows promising results. Visual impairments are observed in psychosis in addition to many neurologic disorders and reflected in abnormalities in retinal layers, seen with the use of OCT. Because of the connection between retinal layers and the thalamus and its higher order projections, ocular biomarkers may shed light on early degenerative mechanisms in psychosis. Furthermore, they may reflect pathophysiologies without the need to image with an MRI, which is both costly and time-consuming.

From an initial meta-analysis of twelve articles, the RNFL, GCL-IPL, and choroid showed significant reductions in thickness. An initial pilot study found reductions in the

RNFL and ONL, as well increases in the OPL. Thinning seen within the RNFL and OPL reflect neuronal synaptic atrophy, and remodeling observed from increased OPL thickness may demonstrate pathologic neuro-inflammatory mechanisms.

Finally, thesis has shown the need for further investigations in retinal cytoarchitectural changes in SZ and BD. Increasing the sample size from this pilot study would increase power and allow for more definitive conclusions from the results. Furthermore, analyzing structural connectivity between the LGN of the thalamus and thalamic projections and retinal layer measures would illuminate RTSD and the mechanisms by which it works.

APPENDIX

Appendix Table 1: PRISMA Guidelines.

	#	Checklist item	Reported on page #
TITLE			
Title	1	Identify the report as a systematic review, meta-analysis, or both.	1
ABSTRACT			
Structured summary	2	Provide a structured summary including, as applicable: background; objectives; data sources; study eligibility criteria, participants, and interventions; study appraisal and synthesis methods; results; limitations; conclusions and implications of key findings; systematic review registration number.	2
INTRODUCTION			
Rationale	3	Describe the rationale for the review in the context of what is already known.	3-4
Objectives	4	Provide an explicit statement of questions being addressed with reference to participants, interventions, comparisons, outcomes, and study design (PICOS).	4
METHODS			
Protocol and registration	5	Indicate if a review protocol exists, if and where it can be accessed (e.g., Web address), and, if available, provide registration information including registration number.	n/a
Eligibility criteria	6	Specify study characteristics (e.g., PICOS, length of follow-up) and report characteristics (e.g., years considered, language, publication status) used as criteria for eligibility, giving rationale.	4
Information sources	7	Describe all information sources (e.g., databases with dates of coverage, contact with study authors to identify additional studies) in the search and date last searched.	4
Search	8	Present full electronic search strategy for at least one database, including any limits used, such that it could be repeated.	4
Study selection	9	State the process for selecting studies (i.e., screening, eligibility, included in systematic review, and, if applicable, included in the meta-analysis).	4
Data collection process	10	Describe method of data extraction from reports (e.g., piloted forms, independently, in duplicate) and any processes for obtaining and confirming data from investigators.	5
Data items	11	List and define all variables for which data were sought (e.g., PICOS, funding sources) and any assumptions and simplifications made.	5-6
Risk of bias in individual studies	12	Describe methods used for assessing risk of bias of individual studies (including specification of whether this was done at the study or outcome level), and how this information is to be used in any data synthesis.	5-6
Summary measures	13	State the principal summary measures (e.g., risk ratio, difference in means).	5-6
Synthesis of results	14	Describe the methods of handling data and combining results of studies, if done, including measures of consistency (e.g., I^2) for each meta-analysis.	5-6
Risk of bias across studies	15	Specify any assessment of risk of bias that may affect the cumulative evidence (e.g., publication bias, selective reporting within studies).	5-6
Additional analyses	16	Describe methods of additional analyses (e.g., sensitivity or subgroup analyses, meta-regression), if done, indicating which were pre-specified.	5-6
RESULTS			
Study selection	17	Give numbers of studies screened, assessed for eligibility, and included in the review, with reasons for exclusions at each stage, ideally with a flow diagram.	6
Study characteristics	18	For each study, present characteristics for which data were extracted (e.g., study size, PICOS, follow-up period) and provide the citations.	6
Risk of bias within studies	19	Present data on risk of bias of each study and, if available, any outcome level assessment (see item 12).	6-9
Results of individual studies	20	For all outcomes considered (benefits or harms), present, for each study: (a) simple summary data for each intervention group (b) effect estimates and confidence intervals, ideally with a forest plot.	6-9
Synthesis of results	21	Present results of each meta-analysis done, including confidence intervals and measures of consistency.	6-9
Risk of bias across studies	22	Present results of any assessment of risk of bias across studies (see Item 15).	6-9
Additional analysis	23	Give results of additional analyses, if done (e.g., sensitivity or subgroup analyses, meta-regression [see Item 16]).	6-9
DISCUSSION			
Summary of evidence	24	Summarize the main findings including the strength of evidence for each main outcome; consider their relevance to key groups (e.g., healthcare providers, users, and policy makers).	10-15
Limitations	25	Discuss limitations at study and outcome level (e.g., risk of bias), and at review-level (e.g., incomplete retrieval of identified research, reporting bias).	15
Conclusions	26	Provide a general interpretation of the results in the context of other evidence, and implications for future research.	10-15
FUNDING			
Funding	27	Describe sources of funding for the systematic review and other support (e.g., supply of data); role of funders for the systematic review.	15

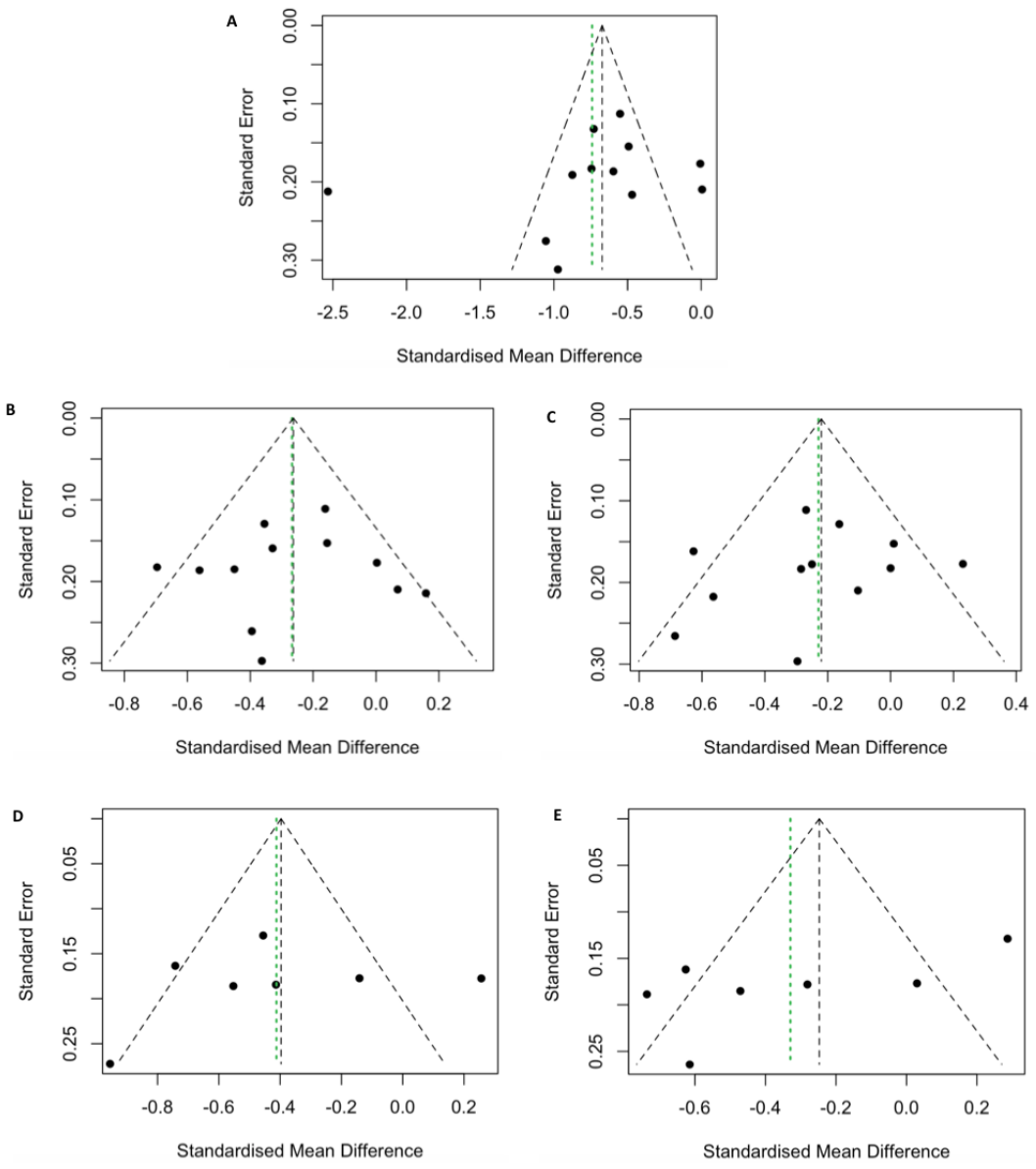

Appendix Figure 1: RNFL funnel plots. Funnels plots are for (A) overall, (B) nasal, (C) temporal, (D) superior, and (E) inferior RNFL regions in probands compared to controls. The green line indicates the overall effect from the proband group.

Table 2: Meta-regression results for RNFL, GCL-IPL, and CT.

	RNFL			GCL-IPL			CT		
Moderator	**beta**	**95% CI**	**P-value**	**beta**	**95% CI**	**P-value**	**beta**	**95% CI**	**P-value**
OCT Device	0.015	-0.31 to 0.34	0.92	-0.096	-0.36 to 0.17	0.26	-0.079	-0.96 to 0.80	0.74
Age probands	0.032	-0.04 to 0.09	0.31	-0.005	-0.08 to 0.07	0.80	-0.011	-0.14 to 0.12	0.75
Age controls	0.019	-0.05 to 0.09	0.55	-0.005	-0.09 to 0.08	0.84	-0.004	-0.13 to 0.12	0.91
% Women probands	-0.008	-0.04 to 0.03	0.62	0.007	-0.01 to 0.03	0.27	0.009	-0.03 to 0.05	0.39
% Women controls	0.003	-0.03 to 0.04	0.85	0.007	-0.03 to 0.05	0.53	0.008	-0.04 to 0.06	0.55
NOS	-0.61	-1.45 to 0.22	0.13	0.25	-0.29 to 0.78	0.18	0.21	-1.05 to 1.47	0.55
Illness Duration (years)	0.0004	-0.06 to 0.06	0.99	-	-	-	-0.070	-0.18 to 0.04	0.12

Note: Data are presented as mean beta values, 95% CI, and p-value. Illness duration for GCL-IPL could not be performed due to small number of studies (n=2). OCT, Optical Coherence Tomography; NOS, Newcastle-Ottawa Scale.

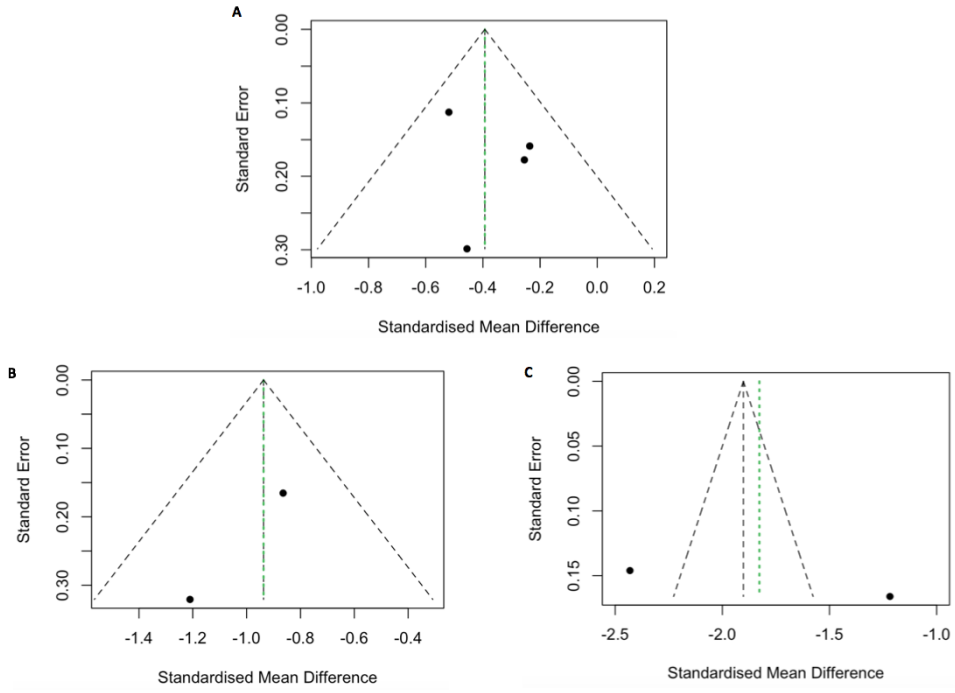

Appendix Figure 2: Ganglion cell layer funnel plots. Funnels plots are for (A) GCL-IPL, (B) GCC, and (C) GCL regions in probands compared to controls. The green line indicates the overall effect from the proband group.

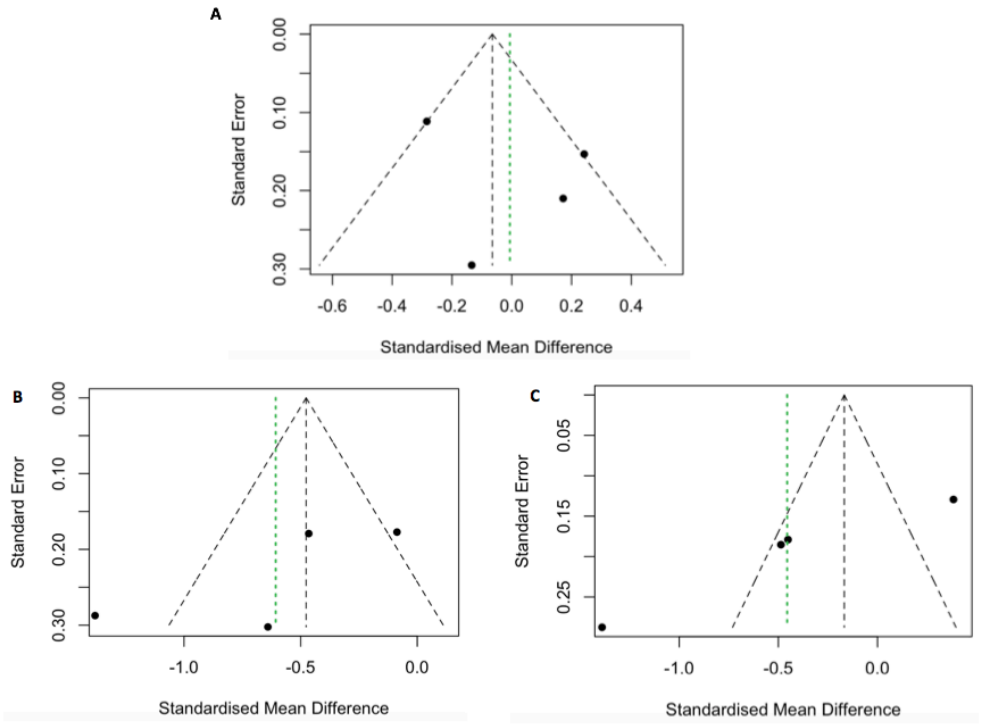

Appendix Figure 3: Funnel plots for choroid and macula regions. Funnels plots are for (A) CT, (B) MT, and (C) MV regions in probands compared to controls. The green line indicates the overall effect from the proband group.

Appendix Table 3: Retinal layer thickness measures in mean eyes for probands, SZ, and BD.

		Probands			SZ			BD		
		t statistic	p Value	Adjusted p Value	t statistic	p Value	Adjusted p Value	t statistic	p Value	Adjusted p Value
Total Retinal	Overall	-0.28	0.78	0.82	-0.01	0.99	0.99	0.40	0.69	0.75
	Inner	-0.22	0.82	0.82	-0.08	0.93	0.99	0.32	0.75	0.75
	Outer	-0.38	0.71	0.82	-0.06	0.95	0.99	0.56	0.59	0.75
	Central	0.56	0.58	0.82	0.83	0.41	0.99	-1.08	0.30	0.75
RNFL	Overall	-1.72	0.10	0.61	-1.99	0.06	0.35	-0.25	0.81	0.94
	Inner	-0.87	0.39	0.72	-1.55	0.14	0.54	-0.16	0.87	0.94
	Outer	-1.55	0.13	0.61	-1.70	0.10	0.49	-0.17	0.87	0.94
	Central	-1.13	0.27	0.61	0.34	0.74	0.94	-2.08	0.06	0.87
GCL	Overall	-1.15	0.26	0.61	-0.71	0.48	0.94	-0.30	0.77	0.94
	Inner	-1.27	0.22	0.61	-0.86	0.40	0.94	-0.21	0.83	0.94
	Outer	-0.96	0.34	0.69	-0.55	0.59	0.94	-0.23	0.82	0.94
	Central	-0.09	0.93	0.97	0.39	0.70	0.94	-1.38	0.19	0.87
IPL	Overall	1.12	0.27	0.61	0.56	0.58	0.94	1.26	0.23	0.87
	Inner	-1.10	0.28	0.61	-1.25	0.22	0.76	0.46	0.66	0.94
	Outer	1.47	0.15	0.61	0.91	0.37	0.94	1.22	0.24	0.87
	Central	-0.44	0.66	0.85	-0.26	0.80	0.94	-0.57	0.58	0.94
INL	Overall	-0.39	0.70	0.85	-0.58	0.57	0.94	1.23	0.24	0.87
	Inner	0.55	0.59	0.83	0.09	0.93	0.97	1.20	0.25	0.87
	Outer	-0.69	0.49	0.83	-0.80	0.43	0.94	0.97	0.35	0.94
	Central	0.61	0.55	0.83	0.30	0.77	0.94	-0.14	0.89	0.94
OPL	Overall	1.98	0.06	0.61	2.82	0.01	0.11	0.17	0.87	0.94
	Inner	1.61	0.12	0.61	2.18	0.04	0.32	0.13	0.90	0.94
	Outer	2.04	0.05	0.61	2.87	0.01	0.11	0.04	0.96	0.96
	Central	-0.03	0.98	0.98	-0.02	0.99	0.99	0.39	0.70	0.94
ONL	Overall	-0.38	0.71	0.85	-0.26	0.80	0.94	-0.84	0.42	0.94
	Inner	-0.25	0.81	0.88	-0.21	0.83	0.94	-0.56	0.58	0.94
	Outer	-0.60	0.55	0.83	-0.38	0.71	0.94	-1.23	0.24	0.87
	Central	0.27	0.79	0.88	0.18	0.86	0.94	0.23	0.82	0.94

Appendix Table 4: Retinal layer thickness measures in right eyes for probands, SZ, and BD.

		Probands			SZ			BD		
		t statistic	p Value	Adjusted p Value	t statistic	p Value	Adjusted p Value	t statistic	p Value	Adjusted p Value
Total Retinal	Overall	-0.44	0.67	1.00	-0.51	0.61	1.00	-0.17	0.87	1.00
	Inner	-0.16	0.87	1.00	0.02	0.99	1.00	-0.23	0.82	1.00
	Outer	-0.71	0.49	1.00	-0.74	0.47	1.00	-0.21	0.84	1.00
	Central	0.62	0.54	1.00	0.89	0.38	1.00	-1.42	0.18	1.00
RNFL	Overall	-0.59	0.56	1.00	-1.38	0.18	1.00	1.22	0.25	1.00
	Inner	-0.27	0.79	1.00	-1.54	0.14	1.00	1.42	0.18	1.00
	Outer	-0.57	0.57	1.00	-1.25	0.22	1.00	1.18	0.26	1.00
	Central	-1.07	0.29	1.00	0.32	0.75	1.00	-1.95	0.07	1.00
GCL	Overall	0.21	0.83	1.00	0.45	0.66	1.00	-0.16	0.88	1.00
	Inner	-0.04	0.96	1.00	0.49	0.63	1.00	-0.51	0.62	1.00
	Outer	0.20	0.84	1.00	0.42	0.68	1.00	-0.10	0.92	1.00
	Central	-0.47	0.64	1.00	0.01	0.99	1.00	-1.37	0.20	1.00
IPL	Overall	0.66	0.52	1.00	0.83	0.41	1.00	-0.07	0.94	1.00
	Inner	-0.09	0.93	1.00	0.33	0.75	1.00	-0.55	0.59	1.00
	Outer	0.92	0.37	1.00	1.00	0.33	1.00	0.35	0.73	1.00
	Central	-0.38	0.71	1.00	-0.25	0.81	1.00	-0.53	0.60	1.00
INL	Overall	0.33	0.74	1.00	0.11	0.91	1.00	-0.04	0.97	1.00
	Inner	-0.15	0.88	1.00	-0.55	0.59	1.00	-0.24	0.81	1.00
	Outer	0.81	0.43	1.00	1.10	0.28	1.00	0.14	0.89	1.00
	Central	0.16	0.88	1.00	0.00	1.00	1.00	-0.64	0.54	1.00
OPL	Overall	1.15	0.26	1.00	1.12	0.27	1.00	0.41	0.69	1.00
	Inner	1.05	0.30	1.00	0.95	0.35	1.00	0.58	0.57	1.00
	Outer	0.75	0.46	1.00	0.60	0.55	1.00	0.32	0.75	1.00
	Central	-0.07	0.95	1.00	0.07	0.95	1.00	-0.03	0.98	1.00
ONL	Overall	-1.41	0.17	1.00	-1.23	0.23	1.00	-1.27	0.23	1.00
	Inner	-1.29	0.21	1.00	-1.16	0.26	1.00	-1.06	0.31	1.00
	Outer	-0.99	0.33	1.00	-0.67	0.51	1.00	-1.54	0.15	1.00
	Central	-0.10	0.92	1.00	-0.23	0.82	1.00	0.14	0.89	1.00

Appendix Table 5: Retinal layer thickness measures in mean eyes for probands, SZ, and BD.

		Probands			SZ			BD		
		t statistic	p Value	Adjusted p Value	t statistic	p Value	Adjusted p Value	t statistic	p Value	Adjusted p Value
Total Retinal	Overall	-0.09	0.93	0.96	0.19	0.85	0.96	-0.77	0.46	0.96
	Inner	-0.24	0.81	0.96	0.12	0.91	0.96	-0.87	0.40	0.96
	Outer	-0.24	0.81	0.96	0.12	0.91	0.96	-0.87	0.40	0.96
	Central	0.46	0.65	0.96	0.72	0.48	0.83	-0.76	0.46	0.73
RNFL	Overall	-0.17	0.87	0.98	-1.42	0.17	0.86	1.58	0.14	0.49
	Inner	0.08	0.94	0.98	-1.33	0.20	0.86	2.03	0.07	0.49
	Outer	0.08	0.94	0.96	-1.33	0.20	0.96	2.03	0.07	0.49
	Central	-1.10	0.28	0.96	0.34	0.74	0.96	-2.03	0.07	0.96
GCL	Overall	0.14	0.89	0.96	0.54	0.59	0.96	-0.35	0.73	0.96
	Inner	0.12	0.91	0.96	0.62	0.54	0.96	-0.40	0.69	0.96
	Outer	0.12	0.91	0.96	0.62	0.54	0.96	-0.40	0.69	0.94
	Central	0.29	0.77	0.96	0.75	0.46	0.96	-1.28	0.23	0.96
IPL	Overall	0.21	0.83	0.96	0.71	0.48	0.96	-0.63	0.54	0.96
	Inner	0.27	0.79	0.96	0.88	0.39	0.96	-0.61	0.55	0.96
	Outer	0.27	0.79	0.96	0.88	0.39	0.96	-0.61	0.55	0.96
	Central	-0.49	0.63	0.96	-0.29	0.78	0.96	-0.62	0.55	0.98
INL	Overall	0.49	0.63	0.96	0.48	0.63	0.96	0.05	0.96	1.00
	Inner	0.38	0.71	0.96	0.42	0.68	0.96	0.00	1.00	1.00
	Outer	0.38	0.71	0.96	0.42	0.68	0.96	0.00	1.00	0.96
	Central	1.07	0.29	0.49	0.63	0.54	0.47	0.50	0.63	0.96
OPL	Overall	2.08	0.05	0.49	2.56	0.02	0.47	0.45	0.66	0.96
	Inner	2.08	0.05	0.49	2.57	0.02	0.47	0.40	0.70	0.96
	Outer	2.08	0.05	0.96	2.57	0.02	0.96	0.40	0.70	0.96
	Central	-0.25	0.80	0.59	0.13	0.90	0.49	-0.41	0.69	0.96
ONL	Overall	-1.66	0.11	0.49	-1.88	0.07	0.49	-0.68	0.51	0.96
	Inner	-1.80	0.08	0.49	-2.03	0.05	0.49	-0.74	0.48	0.96
	Outer	-1.80	0.08	0.96	-2.03	0.05	0.96	-0.74	0.48	0.96
	Central	0.67	0.51	0.96	0.64	0.53	0.96	0.27	0.79	0.96

Appendix Table 6: Statistics data for illness duration correlation with retinal layer measures.

	Subregion	t	p	FDR-Adjusted p
Retinal	Overall	0.89	0.41	0.98
	Inner	-0.08	0.94	0.98
	Outer	0.65	0.54	0.98
	Central	0.02	0.98	0.98
RNFL	Overall	-0.29	0.78	0.98
	Inner	-0.71	0.50	0.98
	Outer	0.38	0.71	0.98
	Central	0.05	0.96	0.98
GCL	Overall	-1.23	0.26	0.98
	Inner	0.02	0.98	0.98
	Outer	-1.22	0.26	0.98
	Central	0.04	0.97	0.98
IPL	Overall	-0.68	0.52	0.98
	Inner	-0.24	0.82	0.98
	Outer	-0.19	0.86	0.98
	Central	-0.27	0.79	0.98
INL	Overall	-1.15	0.29	0.98
	Inner	0.34	0.75	0.98
	Outer	-1.64	0.14	0.98
	Central	-0.85	0.42	0.98
OPL	Overall	-1.48	0.18	0.98
	Inner	-0.96	0.37	0.98
	Outer	-1.21	0.26	0.98
	Central	0.13	0.90	0.98
ONL	Overall	-1.07	0.32	0.98
	Inner	-0.06	0.96	0.98
	Outer	-1.01	0.35	0.98
	Central	-0.58	0.58	0.98

Appendix Table 7: Statistics data for PANSS total score correlation with retinal layer measures.

	Subregion	t	p	FDR-Adjusted p
Retinal	Overall	1.47	0.18	0.52
	Inner	1.21	0.26	0.52
	Outer	0.81	0.44	0.59
	Central	0.21	0.84	0.84
RNFL	Overall	-1.72	0.12	0.78
	Inner	-1.72	0.12	0.78
	Outer	-1.38	0.20	0.78
	Central	0.02	0.98	0.98
GCL	Overall	-1.35	0.21	0.78
	Inner	-1.35	0.21	0.78
	Outer	-0.79	0.45	0.78
	Central	-0.90	0.39	0.78
IPL	Overall	-0.97	0.36	0.78
	Inner	-1.42	0.19	0.78
	Outer	0.05	0.96	0.98
	Central	-0.89	0.40	0.78
INL	Overall	-0.75	0.48	0.78
	Inner	-0.50	0.63	0.79
	Outer	-0.73	0.49	0.78
	Central	-1.30	0.23	0.78
OPL	Overall	-0.65	0.53	0.78
	Inner	-0.35	0.73	0.88
	Outer	-0.54	0.60	0.79
	Central	-0.17	0.87	0.98
ONL	Overall	-0.61	0.56	0.78
	Inner	-0.78	0.46	0.78
	Outer	-0.08	0.94	0.98
	Central	-0.70	0.50	0.78

Appendix Table 8: Statistics data for PANSS negative symptom score correlation with retinal layer measures.

	Subregion	t	p	FDR-Adjusted p
Retinal	Overall	0.74	0.48	0.50
	Inner	0.74	0.48	0.50
	Outer	0.80	0.45	0.50
	Central	0.71	0.50	0.50
RNFL	Overall	-0.36	0.72	0.83
	Inner	-0.98	0.35	0.50
	Outer	-0.02	0.98	0.98
	Central	-1.90	0.09	0.39
GCL	Overall	-2.33	0.05	0.39
	Inner	-1.92	0.09	0.39
	Outer	-1.91	0.09	0.39
	Central	-1.53	0.16	0.39
IPL	Overall	-1.22	0.26	0.41
	Inner	-1.59	0.15	0.39
	Outer	-0.57	0.58	0.73
	Central	-1.24	0.25	0.41
INL	Overall	-1.48	0.18	0.39
	Inner	-1.23	0.25	0.41
	Outer	-1.34	0.22	0.41
	Central	-1.48	0.18	0.39
OPL	Overall	-0.53	0.61	0.73
	Inner	-0.10	0.92	0.96
	Outer	-0.91	0.39	0.52
	Central	-0.32	0.76	0.83
ONL	Overall	-1.60	0.15	0.39
	Inner	-1.53	0.16	0.39
	Outer	-1.98	0.08	0.39
	Central	-0.98	0.36	0.50

Appendix Table 9: Statistics data for PANSS positive symptom score correlation with retinal layer measures.

	Subregion	t	p	FDR-Adjusted p
Retinal	Overall	-0.22	0.83	0.90
	Inner	-0.13	0.90	0.90
	Outer	-0.92	0.39	0.77
	Central	-1.17	0.28	0.77
RNFL	Overall	-0.43	0.68	0.80
	Inner	-0.22	0.83	0.87
	Outer	-0.39	0.71	0.80
	Central	1.51	0.17	0.80
GCL	Overall	0.50	0.63	0.80
	Inner	0.76	0.47	0.80
	Outer	0.36	0.73	0.80
	Central	0.37	0.72	0.80
IPL	Overall	0.66	0.53	0.80
	Inner	0.56	0.59	0.80
	Outer	1.04	0.33	0.80
	Central	0.41	0.70	0.80
INL	Overall	1.18	0.27	0.80
	Inner	1.28	0.24	0.80
	Outer	0.96	0.37	0.80
	Central	0.17	0.87	0.87
OPL	Overall	1.06	0.32	0.80
	Inner	1.10	0.30	0.80
	Outer	1.15	0.28	0.80
	Central	1.29	0.23	0.80
ONL	Overall	0.89	0.40	0.80
	Inner	0.63	0.55	0.80
	Outer	1.70	0.13	0.80
	Central	0.73	0.49	0.80

Appendix Table 10: Statistics data for antipsychotic dosage correlation with retinal layer measures.

	Subregion	t	p	FDR-Adjusted p
Retinal	Overall	2.42	0.06	0.17
	Inner	1.84	0.12	0.17
	Outer	0.73	0.50	0.50
	Central	1.87	0.12	0.17
RNFL	Overall	-0.58	0.59	0.74
	Inner	-1.02	0.35	0.71
	Outer	0.54	0.61	0.74
	Central	-0.40	0.71	0.74
GCL	Overall	-0.89	0.41	0.74
	Inner	-0.64	0.55	0.74
	Outer	-0.44	0.68	0.74
	Central	1.09	0.33	0.71
IPL	Overall	-2.27	0.07	0.71
	Inner	-1.03	0.35	0.71
	Outer	-2.28	0.07	0.71
	Central	-0.21	0.84	0.84
INL	Overall	-1.21	0.28	0.71
	Inner	-1.39	0.22	0.71
	Outer	-0.49	0.65	0.74
	Central	-0.53	0.62	0.74
OPL	Overall	-1.66	0.16	0.71
	Inner	-1.17	0.30	0.71
	Outer	-0.71	0.51	0.74
	Central	-1.64	0.16	0.71
ONL	Overall	-1.47	0.20	0.71
	Inner	-1.29	0.25	0.71
	Outer	-0.80	0.46	0.74
	Central	-0.72	0.50	0.74

Appendix Table 11: Statistics data for smoking status correlation with retinal layer measures.

	Subregion	t	p	FDR-Adjusted p
Retinal	Overall	0.54	0.59	0.79
	Inner	0.26	0.80	0.80
	Outer	0.54	0.59	0.79
	Central	0.76	0.45	0.79
RNFL	Overall	-0.84	0.41	0.81
	Inner	-0.39	0.70	0.89
	Outer	-0.86	0.40	0.81
	Central	-1.11	0.27	0.81
GCL	Overall	-1.40	0.17	0.81
	Inner	-0.70	0.49	0.81
	Outer	-1.58	0.12	0.81
	Central	-1.57	0.12	0.81
IPL	Overall	-0.16	0.87	0.91
	Inner	-0.74	0.46	0.81
	Outer	0.53	0.60	0.85
	Central	-1.66	0.11	0.81
INL	Overall	-0.96	0.34	0.81
	Inner	0.01	0.99	0.99
	Outer	-1.25	0.22	0.81
	Central	-1.35	0.19	0.81
OPL	Overall	0.31	0.76	0.89
	Inner	1.02	0.32	0.81
	Outer	-0.24	0.81	0.89
	Central	0.59	0.56	0.84
ONL	Overall	-0.67	0.51	0.81
	Inner	-0.28	0.78	0.89
	Outer	-0.86	0.40	0.81
	Central	-0.45	0.65	0.87

Appendix Table 12: Statistics data for cortical correlations with retinal layer measures.

		Gray Matter Thickness			Gray Matter Volume			Intra-Cranial Volume		
	Subregion	t	p	FDR-Adjusted p	t	p	FDR-Adjusted p	t	p	FDR-Adjusted p
Retinal	Overall	0.73	0.47	0.71	0.26	0.80	0.89	1.23	0.23	0.70
	Inner	0.77	0.45	0.71	0.90	0.38	0.71	1.70	0.10	0.46
	Outer	-0.10	0.92	0.92	0.95	0.36	0.71	1.92	0.07	0.46
	Central	0.23	0.82	0.89	0.51	0.61	0.82	1.65	0.11	0.46
RNFL	Overall	-1.13	0.27	0.77	1.28	0.22	0.77	0.36	0.72	0.97
	Inner	-2.17	0.04	0.77	0.37	0.71	0.97	0.01	0.99	1.00
	Outer	-0.46	0.65	0.97	0.97	0.35	0.77	0.03	0.97	1.00
	Central	0.00	1.00	1.00	-0.16	0.87	0.97	-0.14	0.89	0.97
GCL	Overall	-1.24	0.23	0.77	-0.72	0.48	0.90	-1.02	0.32	0.77
	Inner	-1.29	0.21	0.77	-1.32	0.20	0.77	-1.01	0.32	0.77
	Outer	-0.79	0.44	0.88	-1.14	0.27	0.77	-1.76	0.09	0.77
	Central	-0.25	0.80	0.97	-0.73	0.47	0.90	-0.02	0.99	1.00
IPL	Overall	-0.99	0.33	0.77	0.18	0.86	0.97	-0.48	0.64	0.97
	Inner	-1.23	0.23	0.77	-1.42	0.17	0.77	-1.36	0.19	0.77
	Outer	-0.44	0.67	0.97	0.43	0.67	0.97	-0.50	0.62	0.97
	Central	-0.45	0.65	0.97	-1.02	0.32	0.77	-0.17	0.87	0.97
INL	Overall	-1.02	0.32	0.77	0.26	0.79	0.97	-0.14	0.89	0.97
	Inner	-1.01	0.32	0.77	-0.95	0.35	0.77	-0.88	0.39	0.80
	Outer	-1.76	0.09	0.77	0.34	0.74	0.97	-0.26	0.80	0.97
	Central	-0.02	0.99	1.00	-0.65	0.52	0.94	0.51	0.61	0.97
OPL	Overall	-0.49	0.63	0.97	-1.06	0.30	0.77	-1.83	0.08	0.77
	Inner	-0.38	0.71	0.97	-1.79	0.09	0.77	-2.72	0.01	0.77
	Outer	0.20	0.85	0.97	-0.89	0.38	0.80	-1.35	0.19	0.77
	Central	-0.17	0.87	0.97	-1.03	0.32	0.77	-1.03	0.32	0.77
ONL	Overall	-1.13	0.27	0.77	0.29	0.78	0.97	-0.65	0.52	0.94
	Inner	-1.23	0.23	0.77	-0.17	0.87	0.97	-1.03	0.32	0.77
	Outer	-0.23	0.82	0.97	-0.37	0.72	0.97	-1.42	0.17	0.77
	Central	-1.95	0.07	0.77	0.11	0.91	0.98	-0.02	0.99	1.00

REFERENCES

Almarcegui, C., Dolz, I., Pueyo, V., Garcia, E., Fernandez, F. J., Martin, J., Ara, J. R., & Honrubia, F. (2010). Correlation between functional and structural assessments of the optic nerve and retina in multiple sclerosis patients. *Neurophysiologie Clinique/Clinical Neurophysiology*, *40*(3), 129–135. https://doi.org/10.1016/j.neucli.2009.12.001

American Psychiatric Association (Ed.). (2013). *Diagnostic and statistical manual of mental disorders: DSM-5* (5th ed). American Psychiatric Association.

Aricioglu, F., Ozkartal, C. S., Unal, G., Dursun, S., Cetin, M., & Müller, N. (2016). Neuroinflammation in Schizophrenia: A Critical Review and The Future. *Klinik Psikofarmakoloji Bülteni-Bulletin of Clinical Psychopharmacology*, *26*(4), 429–437. https://doi.org/10.5455/bcp.20161123044657

Ascaso, F. J., Rodriguez-Jimenez, R., Cabezón, L., López-Antón, R., Santabárbara, J., De la Cámara, C., Modrego, P. J., Quintanilla, M. A., Bagney, A., Gutierrez, L., Cruz, N., Cristóbal, J. A., & Lobo, A. (2015). Retinal nerve fiber layer and macular thickness in patients with schizophrenia: Influence of recent illness episodes. *Psychiatry Research*, *229*(1–2), 230–236. https://doi.org/10.1016/j.psychres.2015.07.028

Celik, M., Kalenderoglu, A., Sevgi Karadag, A., Bekir Egilmez, O., Han-Almis, B., & Şimşek, A. (2016). Decreases in ganglion cell layer and inner plexiform layer volumes correlate better with disease severity in schizophrenia patients than retinal nerve fiber layer thickness: Findings from spectral optic coherence tomography. *European Psychiatry*, *32*, 9–15. https://doi.org/10.1016/j.eurpsy.2015.10.006

Chen, Y. (2011). Abnormal Visual Motion Processing in Schizophrenia: A Review of Research Progress. *Schizophrenia Bulletin*, *37*(4), 709–715. https://doi.org/10.1093/schbul/sbr020

Chkonia, E., Roinishvili, M., Reichard, L., Wurch, W., Puhlmann, H., Grimsen, C., Herzog, M. H., & Brand, A. (2012). Patients with functional psychoses show similar visual backward masking deficits. *Psychiatry Research*, *198*(2), 235–240. https://doi.org/10.1016/j.psychres.2012.02.020

Cho, K. I. K., Kwak, Y. B., Hwang, W. J., Lee, J., Kim, M., Lee, T. Y., & Kwon, J. S. (2019). Microstructural Changes in Higher-Order Nuclei of the Thalamus in Patients With First-Episode Psychosis. *Biological Psychiatry*, *85*(1), 70–78. https://doi.org/10.1016/j.biopsych.2018.05.019

Chorostecki, J., Seraji-Bozorgzad, N., Shah, A., Bao, F., Bao, G., George, E., Gorden, V., Caon, C., Frohman, E., Tariq Bhatti, M., & Khan, O. (2015). Characterization of retinal architecture in Parkinson's disease. *Journal of the Neurological Sciences*, *355*(1–2), 44–48. https://doi.org/10.1016/j.jns.2015.05.007

Chu, E. M.-Y., Kolappan, M., Barnes, T. R. E., Joyce, E. M., & Ron, M. A. (2012). A window into the brain: An in vivo study of the retina in schizophrenia using optical coherence tomography. *Psychiatry Research*, *203*(1), 89–94. https://doi.org/10.1016/j.pscychresns.2011.08.011

Das, U. N. (2016). Diabetic macular edema, retinopathy and age-related macular degeneration as inflammatory conditions. *Archives of Medical Science*, *5*, 1142–1157. https://doi.org/10.5114/aoms.2016.61918

de Barros Garcia, J. M. B., Isaac, D. L. C., & Avila, M. (2017). Diabetic retinopathy and OCT angiography: Clinical findings and future perspectives. *International Journal of Retina and Vitreous*, *3*(1). https://doi.org/10.1186/s40942-017-0062-2

DeLisi, L. E., Szulc, K. U., Bertisch, H. C., Majcher, M., & Brown, K. (2006). Understanding structural brain changes in schizophrenia. *Dialogues in Clinical Neuroscience*, *8*(1), 8.

Demirkaya, N., van Dijk, H. W., van Schuppen, S. M., Abràmoff, M. D., Garvin, M. K., Sonka, M., Schlingemann, R. O., & Verbraak, F. D. (2013). Effect of Age on Individual Retinal Layer Thickness in Normal Eyes as Measured With Spectral-Domain Optical Coherence Tomography. *Investigative Opthalmology & Visual Science*, *54*(7), 4934. https://doi.org/10.1167/iovs.13-11913

Dinkin, M. (2017). Trans-synaptic Retrograde Degeneration in the Human Visual System: Slow, Silent, and Real. *Current Neurology and Neuroscience Reports*, *17*(2). https://doi.org/10.1007/s11910-017-0725-2

Dorph-Petersen, K.-A., & Lewis, D. A. (2017). Postmortem structural studies of the thalamus in schizophrenia. *Schizophrenia Research*, *180*, 28–35. https://doi.org/10.1016/j.schres.2016.08.007

Ehrlich, R., Harris, A., & Moss, A. M. (2010). Anatomy and Regulation of the Optical Nerve Blood Flow. In *Encyclopedia of the Eye* (pp. 73–82). Elsevier. https://doi.org/10.1016/B978-0-12-374203-2.00136-6

Fagerström, K.-O. (1978). Measuring degree of physical dependence to tobacco smoking with reference to individualization of treatment. *Addictive Behaviors*, *3*(3–4), 235–241. https://doi.org/10.1016/0306-4603(78)90024-2

Gabilondo, I., Martínez-Lapiscina, E. H., Martínez-Heras, E., Fraga-Pumar, E., Llufriu, S., Ortiz, S., Bullich, S., Sepulveda, M., Falcon, C., Berenguer, J., Saiz, A., Sanchez-Dalmau, B., & Villoslada, P. (2014). Trans-synaptic axonal degeneration in the visual pathway in multiple sclerosis: Axonal Degeneration in MS. *Annals of Neurology*, *75*(1), 98–107. https://doi.org/10.1002/ana.24030

Garcia-Martin, E., Gavin, A., Garcia-Campayo, J., Vilades, E., Orduna, E., Polo, V., Larrosa, J. M., Pablo, L. E., & Satue, M. (2018). VISUAL FUNCTION AND RETINAL CHANGES IN PATIENTS WITH BIPOLAR DISORDER: *Retina*, 1. https://doi.org/10.1097/IAE.0000000000002252

Garcia-Martin, E., Ruiz-de Gopegui, E., León-Latre, M., Otin, S., Altemir, I., Polo, V., Larrosa, J. M., Cipres, M., Casasnovas, J. A., & Pablo, L. E. (2017). Influence of cardiovascular condition on retinal and retinal nerve fiber layer measurements. *PLOS ONE*, *12*(12), e0189929. https://doi.org/10.1371/journal.pone.0189929

Huang, D., Swanson, E. A., Lin, C. P., Schuman, J. S., Stinson, W. G., Chang, W., Hee, M. R., Flotte, T., Gregory, K., & Puliafito, C. A. (2015). *Optical Coherence Tomography*. 12.

Kalenderoglu, A., Sevgi-Karadag, A., Celik, M., Egilmez, O. B., Han-Almis, B., & Ozen, M. E. (2016). Can the retinal ganglion cell layer (GCL) volume be a new marker to detect neurodegeneration in bipolar disorder? *Comprehensive Psychiatry*, *67*, 66–72. https://doi.org/10.1016/j.comppsych.2016.02.005

Kay, S. R., Fiszbein, A., & Opler, L. A. (1987). The Positive and Negative Syndrome Scale (PANSS) for Schizophrenia. *Schizophrenia Bulletin*, *13*(2), 261–276. https://doi.org/10.1093/schbul/13.2.261

Kempton, M. J., Geddes, J. R., Ettinger, U., Williams, S. C. R., & Grasby, P. M. (2008). Meta-analysis, Database, and Meta-regression of 98 Structural Imaging Studies in Bipolar Disorder. *Archives of General Psychiatry*, *65*(9), 1017. https://doi.org/10.1001/archpsyc.65.9.1017

Khalil, M. A., Saleh, A. A., Gohar, S. M., Khalil, D. H., & Said, M. (2017). Optical coherence tomography findings in patients with bipolar disorder. *Journal of Affective Disorders*, *218*, 115–122. https://doi.org/10.1016/j.jad.2017.04.055

Kromer, R., Tigges, E., Rashed, N., Pein, I., Klemm, M., & Blankenberg, S. (2018). Association between optical coherence tomography based retinal microvasculature characteristics and myocardial infarction in young men. *Scientific Reports*, *8*(1). https://doi.org/10.1038/s41598-018-24083-x

Lee, W. W., Tajunisah, I., Sharmilla, K., Peyman, M., & Subrayan, V. (2013). Retinal Nerve Fiber Layer Structure Abnormalities in Schizophrenia and Its Relationship to Disease State: Evidence From Optical Coherence Tomography. *Investigative Opthalmology & Visual Science*, *54*(12), 7785. https://doi.org/10.1167/iovs.13-12534

Li, X., & Xu, H. (2007). Evidence for Neuroprotective Effects of Antipsychotic Drugs: Implications for the Pathophysiology and Treatment of Schizophrenia. In *International Review of Neurobiology* (Vol. 77, pp. 107–142). Elsevier. https://doi.org/10.1016/S0074-7742(06)77004-0

Lizano, P., Bannai, D., Lutz, O., Kim, L. A., Miller, J., & Keshavan, M. (2020). A Meta-analysis of Retinal Cytoarchitectural Abnormalities in Schizophrenia and Bipolar Disorder. *Schizophrenia Bulletin*, *46*(1), 43–53. https://doi.org/10.1093/schbul/sbz029

London, A., Benhar, I., & Schwartz, M. (2013). The retina as a window to the brain—From eye research to CNS disorders. *Nature Reviews Neurology*, *9*(1), 44–53. https://doi.org/10.1038/nrneurol.2012.227

Lu, Y., Li, Z., Zhang, X., Ming, B., Jia, J., Wang, R., & Ma, D. (2010). Retinal nerve fiber layer structure abnormalities in early Alzheimer's disease: Evidence in optical coherence tomography. *Neuroscience Letters*, *480*(1), 69–72. https://doi.org/10.1016/j.neulet.2010.06.006

Mancall, E. L., & Gray, H. (Eds.). (2011). Gray's clinical neuroanatomy: The anatomic basis for clinical neuroscience. *Gray's Anatomy*.

Mehraban, A., Samimi, S. M., Entezari, M., Seifi, M. H., Nazari, M., & Yaseri, M. (2016). Peripapillary retinal nerve fiber layer thickness in bipolar disorder. *Graefe's Archive for Clinical and Experimental Ophthalmology*, *254*(2), 365–371. https://doi.org/10.1007/s00417-015-2981-7

Merikangas, K. R., Akiskal, H. S., Angst, J., Greenberg, P. E., Hirschfeld, R. M. A., Petukhova, M., & Kessler, R. C. (2007). Lifetime and 12-Month Prevalence of Bipolar Spectrum Disorder in the National Comorbidity Survey Replication. *Archives of General Psychiatry*, *64*(5), 543. https://doi.org/10.1001/archpsyc.64.5.543

Moher, D., Liberati, A., Tetzlaff, J., & Altman, D. G. (2009). Preferred Reporting Items for Systematic Reviews and Meta-Analyses: The PRISMA Statement. *PLoS Medicine*, *6*(7), 6.

Moorhead, T. W. J., McKirdy, J., Sussmann, J. E. D., Hall, J., Lawrie, S. M., Johnstone, E. C., & McIntosh, A. M. (2007). Progressive Gray Matter Loss in Patients with Bipolar

Disorder. *Biological Psychiatry*, *62*(8), 894–900. https://doi.org/10.1016/j.biopsych.2007.03.005

Muneer, A. (2016). Bipolar Disorder: Role of Inflammation and the Development of Disease Biomarkers. *Psychiatry Investigation*, *13*(1), 18. https://doi.org/10.4306/pi.2016.13.1.18

Najjar, S., Pearlman, D. M., Alper, K., Najjar, A., & Devinsky, O. (2013). Neuroinflammation and psychiatric illness. *Journal of Neuroinflammation*, *10*(1). https://doi.org/10.1186/1742-2094-10-43

Ng, W. X. D., Lau, I. Y., Graham, S., & Sim, K. (2009). Neurobiological evidence for thalamic, hippocampal and related glutamatergic abnormalities in bipolar disorder: A review and synthesis. *Neuroscience & Biobehavioral Reviews*, *33*(3), 336–354. https://doi.org/10.1016/j.neubiorev.2008.10.001

O'Bryan, R. A., Brenner, C. A., Hetrick, W. P., & O'Donnell, B. F. (2014). Disturbances of visual motion perception in bipolar disorder. *Bipolar Disorders*, *16*(4), 354–365. https://doi.org/10.1111/bdi.12173

Osiac, E., Pirici, I., Ianc, M., Mitran, S. I., & Albu, C. V. (2014). *Optical coherence tomography investigation of ischemic stroke inside a rodent model*. 6.

Petzold, A., Wong, S., & Plant, G. T. (2016). Autoimmunity in visual loss. In *Handbook of Clinical Neurology* (Vol. 133, pp. 353–376). Elsevier. https://doi.org/10.1016/B978-0-444-63432-0.00020-7

Pilat, A., McLean, R. J., Proudlock, F. A., Maconachie, G. D. E., Sheth, V., Rajabally, Y. A., & Gottlob, I. (2016). In Vivo Morphology of the Optic Nerve and Retina in Patients

With Parkinson's Disease. *Investigative Opthalmology & Visual Science*, *57*(10), 4420. https://doi.org/10.1167/iovs.16-20020

Polo, V., Satue, M., Gavin, A., Vilades, E., Orduna, E., Cipres, M., Garcia-Campayo, J., Navarro-Gil, M., Larrosa, J. M., Pablo, L. E., & Garcia-Martin, E. (2018). Ability of swept source OCT to detect retinal changes in patients with bipolar disorder. *Eye*. https://doi.org/10.1038/s41433-018-0261-6

Saidha, S., Sotirchos, E. S., Oh, J., Syc, S. B., Seigo, M. A., Shiee, N., Eckstein, C., Durbin, M. K., Oakley, J. D., Meyer, S. A., Frohman, T. C., Newsome, S., Ratchford, J. N., Balcer, L. J., Pham, D. L., Crainiceanu, C. M., Frohman, E. M., Reich, D. S., & Calabresi, P. A. (2013). Relationships Between Retinal Axonal and Neuronal Measures and Global Central Nervous System Pathology in Multiple Sclerosis. *JAMA Neurology*, *70*(1), 34. https://doi.org/10.1001/jamaneurol.2013.573

Samani, N. N., Proudlock, F. A., Siram, V., Suraweera, C., Hutchinson, C., Nelson, C. P., Al-Uzri, M., & Gottlob, I. (2018). Retinal Layer Abnormalities as Biomarkers of Schizophrenia. *Schizophrenia Bulletin*, *44*(4), 876–885. https://doi.org/10.1093/schbul/sbx130

Schaefer, K. L., Baumann, J., Rich, B. A., Luckenbaugh, D. A., & Zarate, C. A. (2010). Perception of facial emotion in adults with bipolar or unipolar depression and controls. *Journal of Psychiatric Research*, *44*(16), 1229–1235. https://doi.org/10.1016/j.jpsychires.2010.04.024

Silverstein, S. M., & Keane, B. P. (2011). Perceptual Organization Impairment in Schizophrenia and Associated Brain Mechanisms: Review of Research from 2005 to

2010. *Schizophrenia Bulletin*, *37*(4), 690–699. https://doi.org/10.1093/schbul/sbr052

Silverstein, Steven M., Paterno, D., Cherneski, L., & Green, S. (2017). Optical coherence tomography indices of structural retinal pathology in schizophrenia. *Psychological Medicine*, *48*(12), 2023–2033. https://doi.org/10.1017/S0033291717003555

Topcu-Yilmaz, P., Aydin, M., & Cetin Ilhan, B. (2018). Evaluation of retinal nerve fiber layer, macular, and choroidal thickness in schizophrenia: Spectral optic coherence tomography findings. *Psychiatry and Clinical Psychopharmacology*, 1–6. https://doi.org/10.1080/24750573.2018.1426693

Turetsky, B. I., Kohler, C. G., Indersmitten, T., Bhati, M. T., Charbonnier, D., & Gur, R. C. (2007). Facial emotion recognition in schizophrenia:When and why does it go awry? *Schizophrenia Research*, *94*(1–3), 253–263. https://doi.org/10.1016/j.schres.2007.05.001

Walton, E., Hibar, D. P., van Erp, T. G. M., Potkin, S. G., Roiz-Santiañez, R., Crespo-Facorro, B., Suarez-Pinilla, P., van Haren, N. E. M., de Zwarte, S. M. C., Kahn, R. S., Cahn, W., Doan, N. T., Jørgensen, K. N., Gurholt, T. P., Agartz, I., Andreassen, O. A., Westlye, L. T., Melle, I., Berg, A. O., … Ehrlich, S. (2018). Prefrontal cortical thinning links to negative symptoms in schizophrenia via the ENIGMA consortium. *Psychological Medicine*, *48*(01), 82–94. https://doi.org/10.1017/S0033291717001283

Wells, G., Shea, B., O'Connell, D., Peterson, J., Welch, V., Losos, M., & Tugwell, P. (2012). *The Newcastle-Ottowa Scale (NOS) for assessing the quality of nonrandomised*

studies in meta-analysis.

http://www.ohri.ca/programs/clinical_epidemiology/oxford.asp

Yu, J., Feng, Y., Xiang, Y., Huang, J., Savini, G., Parisi, V., Yang, W., & Fu, X. (2014). Retinal Nerve Fiber Layer Thickness Changes in Parkinson Disease: A Meta-Analysis. *PLoS ONE*, *9*(1), e85718. https://doi.org/10.1371/journal.pone.0085718

Zarei, R., Anvari, P., Eslami, Y., Fakhraie, G., Mohammadi, M., Jamali, A., Afarideh, M., Ghajar, A., Heydarzade, S., Esteghamati, A., & Moghimi, S. (2017). Retinal nerve fibre layer thickness is reduced in metabolic syndrome. *Diabetic Medicine: A Journal of the British Diabetic Association*, *34*(8), 1061–1066. https://doi.org/10.1111/dme.13369

CURRICULUM VITAE